國立嘉義大學

光電暨固態電子研究所

碩士論文

National Chiayi University

Graduate Institute of Optoelectronics

and Solid State Electronics

Master Thesis

渺子生命期受原子核捕捉之改變

The muon lifetime variation by nuclei capture

指導教授:李宗隆 博士

Tsung-Lung Li Ph.D

章文箴 博士

Wen-Chen Chang Ph.D

研究生:許軒豪

Shiuan-Hal Shiu

中華民國 九十六 年 七 月

July 2007

摘要

渺子(Muon)為標準模型中所闡述之第二世代的輕子(lepton)，帶負電的渺子其與物質之交互作用乃與物質之原子序的四次方成比例，此渺子受到原子核捕捉之現象會造成渺子生命期的縮短，本論文嘗試利用閃爍探測器(scintillation detector)、時間數位轉換器(Time to Ddigital Cconverter)以及類比數位轉換器(Aanalog to Digital Converter)來分辨渺子與物質交互作用之訊號以及渺子自由衰變之訊號。

Abstract

Muon is the second generation lepton. The interaction probability of negative charged muon and matter is proportional to Z^4, where Z is the atomic number of the nucleus and this leads to the shortening of lifetime for muons captured by nuclei, in comparison with its free-decay one. This thesis is to study this dependence by using scintillation detector, Time to Digital Converter (TDC) and Analog to Digital Converter (ADC) to differentiate the events which are produced by muon interaction with matters or the ones by free decay.

致謝

首先要感謝我的指導教授李宗隆老師以及中央研究院物理研究所的章文箴老師，如果沒有這兩位老師的辛勤指導，這篇論文是不可能有機會出現的，於此致上我最由衷的感謝。

其次，要感謝中研院物理所的鄧炳坤老師，在實驗儀器方面的指導，實在讓我受益良多。家益學長、璨隆學長以及素音在程式寫作以及取數系統上的幫忙，也實在讓我不勝感激。煌時、紹華、清元、竹芸和永勝，感謝你們在各地的幫忙，讓我在嘉義和台北這兩地之間的學習過程輕鬆不少。

最後要感謝家人以及依恆給予我的支持和鼓勵，讓我這段時間能專心於學習和研究上。謹將此論文獻給所有有幫助過我的人，謝謝大家。

Contents

1 Introduction **1**
1.1 Physics Motivation . . . 1

2 Experimental Setup **7**
2.1 Scintillation Detectors . . . 7
2.1.1 General Characteristics . . . 7
2.1.2 Organic Scintillator . . . 8
2.1.3 Light Guide . . . 8
2.1.4 Photomultiplier Tube(PMT) . . . 8
2.2 Specifications of Electronic Device . . . 9
2.2.1 NIM . . . 10
2.2.2 VMEbus . . . 11
2.3 Electronic Device . . . 12
2.3.1 Discriminator . . . 12
2.3.2 Linear Fan-Out . . . 12
2.3.3 Coincidence Unit . . . 12
2.3.4 Gate Generator . . . 13
2.3.5 Time to Digital Converter(TDC) . . . 13
2.3.6 Analog to Digital Converter(ADC) . . . 14

3 Basic Definition and Experiment Setup **17**
3.1 Basic Definition . . . 17
3.1.1 Muon Lifetime . . . 17
3.1.2 Muon Capture . . . 18
3.2 Experiment Setup . . . 18
3.2.1 The Flow Path of Experiment . . . 18
3.2.2 Experiment Setup . . . 19
3.2.3 Data Acquisition(DAQ) System . . . 21
3.3 Calibration of the Experiment Apparatus . . . 22
3.3.1 Calibration of PMT working voltage . . . 22
3.3.2 Calibration of the Efficiency of Electronic Apparatus in Different Time Scale . . . 24

4 Data Analysis and Results Discussion **27**
4.1 Data Analysis Procedure . . . 27
4.1.1 TDC Data Analysis Procedure . . . 27
4.1.2 ADC Data Analysis Procedure . . . 28
4.2 Monte Carlo Simulation . . . 28
4.2.1 Monte Carlo Simulation Result . . . 29
4.3 TDC Data Analysis and Result . . . 32
4.4 ADC Data Analysis and Results . . . 37

5 Conclusion **47**

A Visual Basic Program **49**

B Monte Carlo Simulation Program **53**

List of Figures

1.1 Muon decay involves a W boson. Muon will decay into an electron and two neutrino. . . . 3
1.2 The proton strikes the top atmosphere. The cosmic rays collide with the atom of atmosphere and produce many particles. . . . 4
1.3 The free decay and capture component[1]. The circle dot is the free decay component, and the triangle dot is the captured decay component. . . . 5
1.4 Figure of $\lambda_{cap.}(A,Z)/ < \rho >$ VS. $(A-Z)/2A$.[9]. In this figure $\pi a_0^3 < \rho >= Z_{eff}^4$. 6

2.1 A simply diagram of scintillation detector. The scintillation detector is composed by scintillator, light guide, photomultiplier, and photomultiplier tube base. . . . 7
2.2 An example of photomultiplier tube connecting with a scintillator. The photon emitted by scintillator will transfer by light guide to the PMT photocathode. . . 8
2.3 Light guide made in a form like fish tail. . . . 9
2.4 Schematic diagram of PMT. . . . 10
2.5 A VMEbus crate. We can simply change the module on the crate. . . . 11
2.6 The discriminator will output a digital signal if the input pulse can surpass the threshold. . . . 12
2.7 Basic operation of Linear Fan-out. Linear Fan-out module can clone the pulse. . 13
2.8 The coincidence unit operation. If the input A and B are time coincidence, the module will output a digital signal. If not, the module will output nothing. . . . 13
2.9 The gate generator operation. When the gate generator received a signal, it will output a gate. . . . 14
2.10 Working principle of the TDC. When the TDC received a start signal the internal clock will start count, until the TDC received a stop signal and the TDC will output the clock counts. . . . 14
2.11 Wilkinson method of ADC. The capacitor will start charging when the ADC received a gate. When the gate disappear the capacitor will start discharge and a clock will start running at the same time. When the discharge was done the lock will output it's counts, the counts can tell us the charge information of the input pulse. . . . 15

3.1 The flow path of experiment. . . . 19
3.2 Block diagram of experiment setup. . . . 19
3.3 Structure of detector. In this experiment we use three scintillation detector and a layer of target. . . . 20
3.4 Timing chart of the NIM modules. . . . 21
3.5 ADC and TDC flowchart. . . . 22
3.6 The structure of DAQ system. . . . 23
3.7 The diagram of plateau. In this experiment the suitable PMT working voltage is in plateau region. . . . 23
3.8 Plateau measurement setup. . . . 24

3.9 Coincidence plateau measurement setup. 24
3.10 The plateau measurement results. In (a) and (b) we can not clearly find out the plateau region and in (c) the plateau region is very obvious. 25
3.11 The coincidence plateau measurement results. The counts is constrained by coincidence with PMT3, and we choose the first several point to be the plateau region. 26
3.12 The setup of testing the efficiency of electronic apparatus. 26

4.1 The different vector size in TDC data. The first several bins are cut in a small scale and after it are cut in bigger scale. 28
4.2 Changing end point for free decay. Because the captured events adding in (b), the fitting result have a difference trend between (a) and (b). 29
4.3 Changing start point for free decay. The fitting result in (a) are all the same, but in (b), because the captured events adding the first several points have different fitting result. 30
4.4 The fitting result of Monte Carlo data. The results are consistent with the value we set. We think by this check, we can trust our analysis program. 31
4.5 Results of changing the fitting end point of free decay. This fitting is try to find out the suitable end point for free decay part fitting. 32
4.6 Results of changing the fitting start point of free decay. This fitting is used to find out the suitable start point for free decay part fitting. 33
4.7 Results of fitting. The capture lifetime fitting result of Cu, Fe, and Al target include data are $0.351 \pm 0.084\mu s$, $0.258 \pm 0.094\mu s$, and $0.756 \pm 0.215\mu s$. 35
4.8 The muon free decay lifetime fitting result. This result is fitted by the function $y = C_{free}e^{-t/\tau_{free}} + C_{pedestal}$ which with no capture component. 36
4.9 ADC VS. TDC profile analysis result. This analysis shows all the TDC without any cut. 37
4.10 ADC VS. TDC profile analysis result (TDC$<$ 1000). In order to find out the captured events we focus on the range where TDC$<1000ns$ 38
4.11 The result of probability of compatibility test. In this test, we try to compare the probability of compatibility in different TDC range to find if there is any evidence can separate the captured events and free decay events. 39
4.12 The ADC shape. In this figure the three different color line label the ADC cut point. 40
4.13 Different ADC Cut for the data without target. 42
4.14 Different ADC Cut for the data with Cu target. 43
4.15 Different ADC Cut for the data with Fe target. 44
4.16 Different ADC Cut for the data with Al target. 45

List of Tables

1.1 The characteristics of muon 2
1.2 The muon decay mode 2
1.3 Muon capture lifetime for several atom 5

2.1 The specifications of PMT H6614-70 9
2.2 The electrical specifications of NIM 10
2.3 The specifications of LeCroy 1176 TDC 15
2.4 The specifications of LeCroy 1182 ADC 16

3.1 The working voltage and threshold voltage for detectors. 24

4.1 The results of TDC data analysis. 34
4.2 The results of probability of compatibility between two ADC histogram. 39

Chapter 1

Introduction

In this chapter we will explain the physics motivation of this study will be introduced and discuss the phenomenon of muon decay and muon capture.

1.1 Physics Motivation

Muon is a kind of fundamental particle which observed by S. H. Neddermeyer and C. D. Anderson in 1937 while they studying cosmic ray[2]. They found there were some particles heavier than electron but lighter than proton, and much more penetrating than electron. It was the first discovered elementary particle that did not appear in ordinary atoms. They initially called the new particle a mesotron. The prefix meso- in Greek word means "intermediate". After that, more and more particles with intermediate mass were founded, and group under the meson, the mesotron was renamed to mu(μ) meson. Several years later, more and more knowledge of elementary particles were established, the physicist found that the muon is not the same with other particles, the muon is one part of the basic building blocks of matter. Finally the muon were put under the lepton with electron(e) and tau(τ) and their contrast neutrino.

The muon and electron ,tau and their corresponding neutrinos are classified as lepton. Muon is a second generation lepton with negative charge and a spin of 1/2. It has a mean lifetime of 2.2μsec, longer than other meson, baryon and unstable lepton like tau. Muon has an antimatter partner: the antimuon(μ^+). Antimuon has the same mass and spin but opposite charge. The muon is often denoted by μ^- and antimuons by μ^+.

Muon has the same electric charge of the electron but 206.7 times the electron mass. We can imagine that muon is a heavy electron. As a result of the heavier mass, the muon is much more penetrating than electrons and emit less bremsstrahlung radiation. Table 1.1 are some characteristics of muon.

Muon is a second generation lepton. It must decay to an electron and other particles with a net charge of zero. The muon decays into an electron, a muon-neutrino, and an electron-antineutrino. Antimuon decays into a positron, a muon-antineutrino, and an electron-neutrino. The processes are:

$$\mu^- \rightarrow e^- + \overline{\nu_e} + \nu_\mu \tag{1.1}$$

$$\mu^+ \rightarrow e^+ + \overline{\nu_\mu} + \nu_e \tag{1.2}$$

Fig. 1.1 is the diagram of the most common muon decay.$\mu^- \rightarrow e^- + \overline{\nu_e} + \nu_\mu$is the most common decay mode but there are some other decay modes. Table 1.2 listing the decay modes. The antimuon decay mode are charge conjugates of the modes in the table.

The muon has a rest mass of 105 MeV. If we want to produce it, we must require an available CM frame energy over 105 MeV. Without an accelerator, we can not reach so huge energy. But

Table 1.1: The characteristics of muon.

Symbol	μ^-
Family	Fermion
Group	Lepton
Generation	Second
Mass(MeV/c^2)[3]	$105.6583692 \pm 0.0000094$
Mean lifetime(μsec)[3]	2.19703 ± 0.00004
Charge	$-e$
Spin	1/2
Antiparticle	Antimuon(μ^+)
Interaction	Weak, Electromagnetic, Gravity

Table 1.2: The muon decay mode[3].

	Mode	Fraction(Γ_i/Γ)
1	$\mu^- \to e^- + \overline{\nu_e} + \nu_\mu$	$\approx 100\%$
2	$\mu^- \to e^- + \overline{\nu_e} + \nu_\mu + \gamma$	$1.4 \pm 0.4\%$
3	$\mu^- \to e^- + \overline{\nu_e} + \nu_\mu + e^+ + e^-$	$3.4 \pm 0.4 \times 10^{-5}\%$
4	$\mu^- \to e^- + \nu_e + \overline{\nu_\mu}$	$< 1.2\%$
5	$\mu^- \to e^- + \gamma$	$< 1.2 \times 10^{-11}\%$
6	$\mu^- \to e^- + e^+ + e^-$	$< 1.0 \times 10^{-12}\%$
7	$\mu^- \to e^- + 2\gamma$	$< 7.2 \times 10^{-11}\%$

fortunately, the muons appear frequently on earth .

There are many high energy particles which we call cosmic rays bombard the earth's top atmosphere anytime. The high energy particles produced by the other parts of the universe such as rotating neutron stars, radio galaxies, supernova, and black holes. But we can not fully understand why the high energy particles were produced. The cosmic rays includes many kinds of particles like protons, electrons, and heavier nuclei. Although the combination of the particles depend on the energy, we still can approximate the compose of $\sim 98\%$ nuclei and $\sim 2\%$ electrons and positrons. The nuclear component contains $\sim 87\%$ are hydrogen, $\sim 12\%$helium, and $\sim 1\%$for all other heavier nuclei[7].

The huge amount high energy particle collide with the nuclei at the earth's top atmosphere and produce a shower of particles includes many kinds of particles like protons, neutrons, pions, kaons, positrons, and electrons etc. Fig. 1.2 shows the picture about the proton strike the top atmosphere.

When a cosmic ray proton strike the nuclei of the top atmosphere air atoms, it may create pions. After pion produced it will decay into a muon and a neutrino or an antineutrino immediate. By the theory of relativity, muons which have a relative high speed can travel a long distance from top atmosphere to our detector. The flux of sea level muons is $\approx 1cm^{-2}min^{-1}$

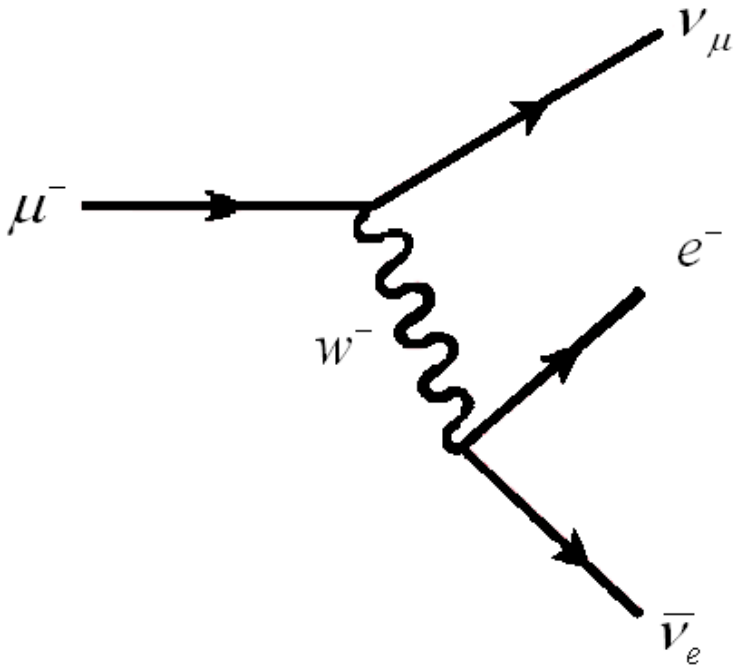

Figure 1.1: Muon decay involves a W boson. Muon will decay into an electron and two neutrino.

for horizontal detectors[6].

When a muon stops in our detector, there are two fates for a muon to disappear. First, muon spontaneously decay into an electron or a positron and two neutrino. The timing between the muon entering the detector and spontaneously decay is called muon lifetime. We can using a detector named scintillation detector and some simple electronic device to measure it.

The scintillation detector can detect the charged particle pass through. When the muon entering the detector, because of its charge, the detector will emit light. After the muon decay into a electron and two neutrinos, the neutrinos have no charge, but the electron is of negative charge then the detector will receive the second signal. We can use some electronic device to get the timing of that two signals.

Why physicists interested in the lifetime of muon?

The physicists are used to describe the world by constant. Like Newton's constant F or the light speed constant c, constants are the common language in physics. There's no exception for weak force. In order to describe the strength of the weak force, physicists defines a constant G_F. By some simple approximation, the relationship between the G_F and muon lifetime τ is $\tau = \frac{192\pi^3\hbar^7}{G_F^2 m^5 c^4}$ here m is the mass of muon.

The second fate of the muon which stopping in the detector is a phenomenon "muon capture." Before introducing muon capture, I want to introduce what is exotic atom first. Exotic atom is an analogue of a normal atom. The difference is one or more of the negative charged electrons are replaced by other negative particles like muons, and negative charged pions or protons are replaced by other positive charged elementary particles, or both. Due to the very short lifetime of this kind particles, exotic atoms often have an extremely short lifetime.

When a muon stops in the matter, muon may be captured by atom's nuclei and transitions down to the K-shell on a short time around 10^{-9}sec to form a muonic atom. In muonic atom, one electron is replaced by negative charged muon. By the electromagnetic force the negative charged muon can bind to the matter's nuclei like electron. Muon have a mass of $105.6 MeV/c^2$ which is 206.7 times to the electron mass. Due to the relatively high mass of muon, when muon

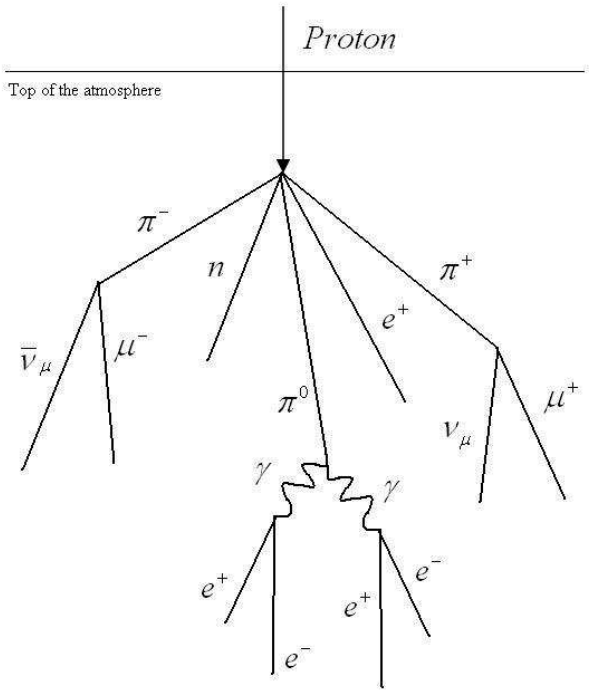

Figure 1.2: The proton strikes the top atmosphere. The cosmic rays collide with the atom of atmosphere and produce many particles.

is bound by nuclei the Bohr radius is 206.7 times smaller than electron orbit. Because of the small orbit, muon may be captured by protons inside the nuclei. The muon capture process is:

$$\mu^- + p \rightarrow n + \nu_\mu \tag{1.3}$$

The above process occurs in a extremely short time around 10^{-14}sec, we can neglect it from the lifetime.

When the capture process occur, the neutron will be emitted, and may be detected by our detector. Although the neutron have zero charge but it still may influence our detector. I'll discuss the influence later. Because the influence of muon capture process, the muon lifetime we measure is an mixture of free decay and capture decay. The capture lifetime is relatively short than the free decay lifetime FIG. 1.3 from[1] shows the free decay and capture component.

The probability for nuclear captured muon is proportional to Z^4, here Z is the atomic number of nuclear. The muon capture rate can express in $\lambda_{cap}(A,Z) = \gamma\lambda_{cap.}(1,1)Z^4_{eff}[\frac{1-(A-Z)\delta}{2A}]$[8]. Here $\lambda_{cap.}$ is the capture decay rate, A is atomic mass, Z is atomic number, $<\rho>$ is effective charge density. Fig. 1.4 shows the world average experiment data about $\lambda_{cap.}$. By the interaction with nuclei, the capture lifetime is shorter than free decay lifetime. Table. 1.3 are some data about the muon lifetime variation by nuclei capture.

In early stage, the electronic apparatus do not have enough timing resolution to separate the muon lifetime in free decay component and capture decay component. Now, the technology has great progress, the modern electronic already have enough timing resolution to separate the two components. In this experiment, we are try to use the modern electronic apparatus to measure the muon capture lifetime, and try to use an ADC module to separate it by pulse energy separation, the details will discuss in this writing.

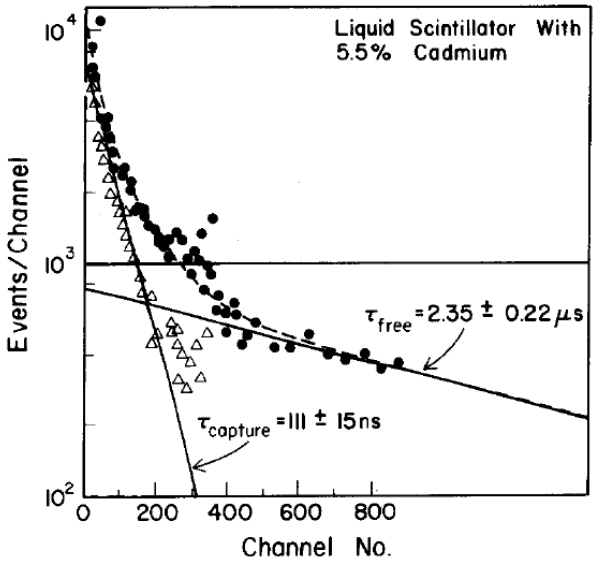

Figure 1.3: The free decay and capture component[1]. The circle dot is the free decay component, and the triangle dot is the captured decay component.

Table 1.3: Muon capture lifetime for several kinds of nuclei[10].

Nucleus	Lifetime(μsec)
Al	0.88 ± 0.011
Fe	0.201 ± 0.004
Cu	0.164 ± 0.002
Ba	0.0945 ± 0.0007
Pb	0.0749 ± 0.0004

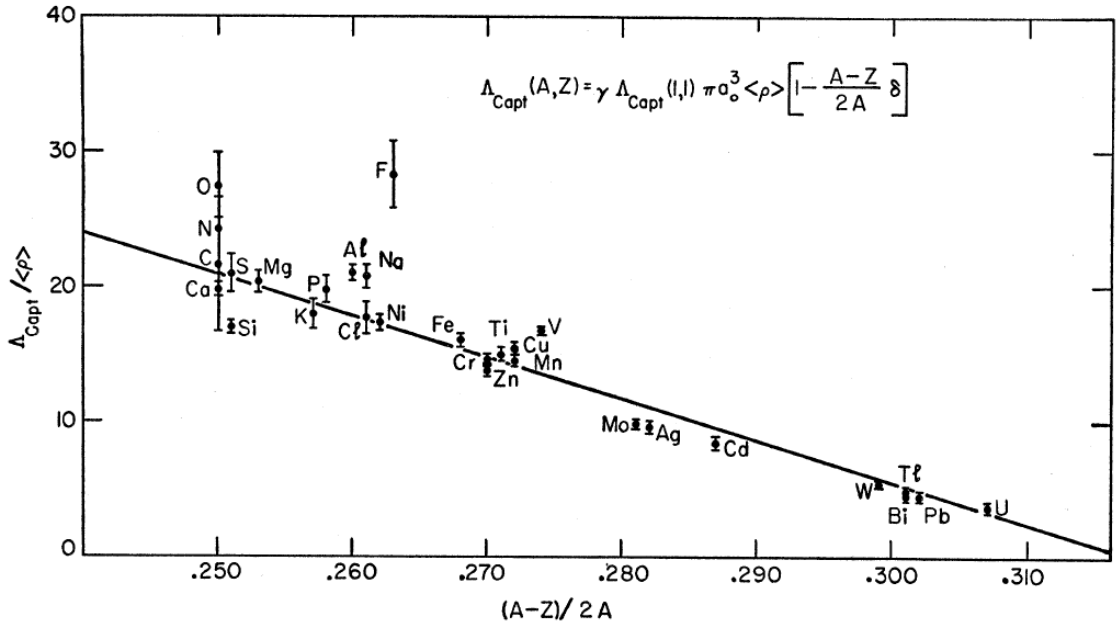

Figure 1.4: Figure of $\lambda_{cap.}(A,Z)/ < \rho >$ VS. $(A-Z)/2A$.[9]. In this figure $\pi a_0^3 < \rho >= Z_{eff}^4$.

Chapter 2

Experimental Setup

This chapter is about the experimental setup. All the experimental apparatus in the experiment will be introduced in this chapter like scintillator, Photomultiplier Tube, Time to Digital Converter, and Analog to Digital Converter etc.

2.1 Scintillation Detectors

Because of the extreme small size and slight energy of the elemental particle, if we want to detect them, we must use some special detector. The scintillation detector is the most widely used fundamental particle detector. It is widely used in nuclear and particle physics today. In this section I'll introduce some characteristic of the scintillation detector.

2.1.1 General Characteristics

Fig. 2.1 shows the general characteristics of scintillation detector. The scintillation detector often consist of a piece of scintillating material and a light guide which optically connected with scintillation material and photomultiplier. And finally, the photomultiplier is connect to a tube base which support the voltage for photomultiplier working and amplified the signal. As the high energy particle passing through the scintillator, it excites the atoms and causes the scintillator emitting some photons. The photons are transmitted by the light guide to the photomultiplier which converts the photons to weak current signal of photoelectrons. Finally the tube base amplified the signal and out put to the BNC connector.

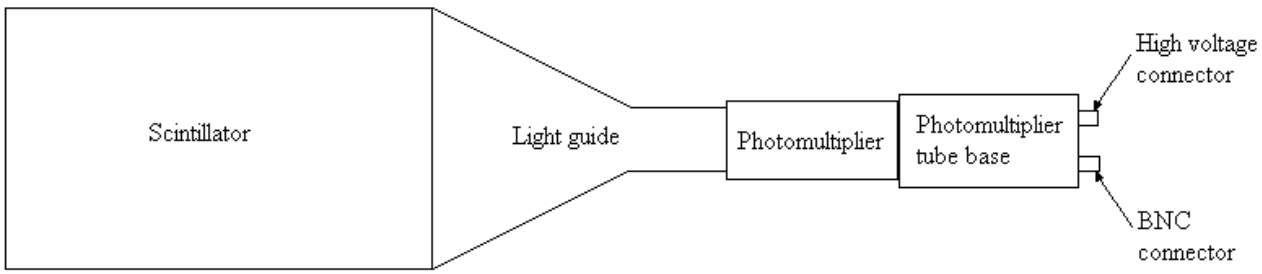

Figure 2.1: A simply diagram of scintillation detector. The scintillation detector is composed by scintillator, light guide, photomultiplier, and photomultiplier tube base.

2.1.2 Organic Scintillator

Generally speaking, there are two kinds of scintillator, organic scintillator, and inorganic scintillator. The organic scintillator includes organic crystals, organic liquids, and plastics scintillator. The inorganic scintillator includes inorganic crystals, gaseous and glasses scintillator.

When a charged particle passing through the scintillator, it will lose energy to excite the scintillator's atom to excited state. After 10^{-8} second, the atom will de-excite to the ground state and emit fluorescence photons. We can use the photomultiplier tube(PMT) to collect the photons and convert it to the electronic signal. I'll introduce the PMT later.

In general, the organic scintillator often have a fast response and short decay time relative to the inorganic scintillator. Because of the excellent property in response and decay time, the organic scintillator often is used to measure the timing and trigger. In this experiment we using the plastic scintillator to be our detector. The plastic scintillators is the most widely used scintillator in organic scintillator, it contains all the advantage of organic scintillator and cheaper than organic crystals, organic liquids scintillator.

2.1.3 Light Guide

In many experiments the scintillator and the photomultiplier tube do not have the same cross section. In order to avoid the light escaping from the scintillator, we use a light guide to couple the photomultiplier tube and the scintillator. From the Fig. 2.2 it can be seen that the light guide connects the scintillator and photomultiplier tube. The light guide usually made of optical quality plastic and made in any shapes and lengths to match the scintillator. The Fig. 2.3 shows that a common design for light guide called "fish tail."

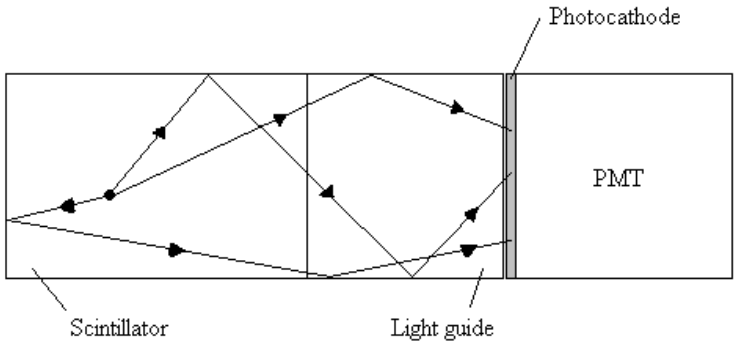

Figure 2.2: An example of photomultiplier tube connecting with a scintillator. The photon emitted by scintillator will transfer by light guide to the PMT photocathode.

2.1.4 Photomultiplier Tube(PMT)

Photomultipliers is a kind of device converting the light into electric pulse. It's widely use in many fields, like optics, nuclear, and high energy physics. Fig. 2.4 is a schematic diagram of PMT. When applying high voltage to the PMT, the photocathode-dynode-anode structure will establish a potential ladder. When an incident photon strikes the photocathode, by photoelectric effect, electrons are emitted. Because of the applied high voltage, the electrons are accelerated to the first dynode. When electrons arrive the dynode, it transfers some of its energy to the electrons in the dynode. This causes secondary electrons to be emitted. After many times of this effect, an electron cascade is created. Finally, the cascade is collected at the anode and give a current which is the signal in analog signal form.

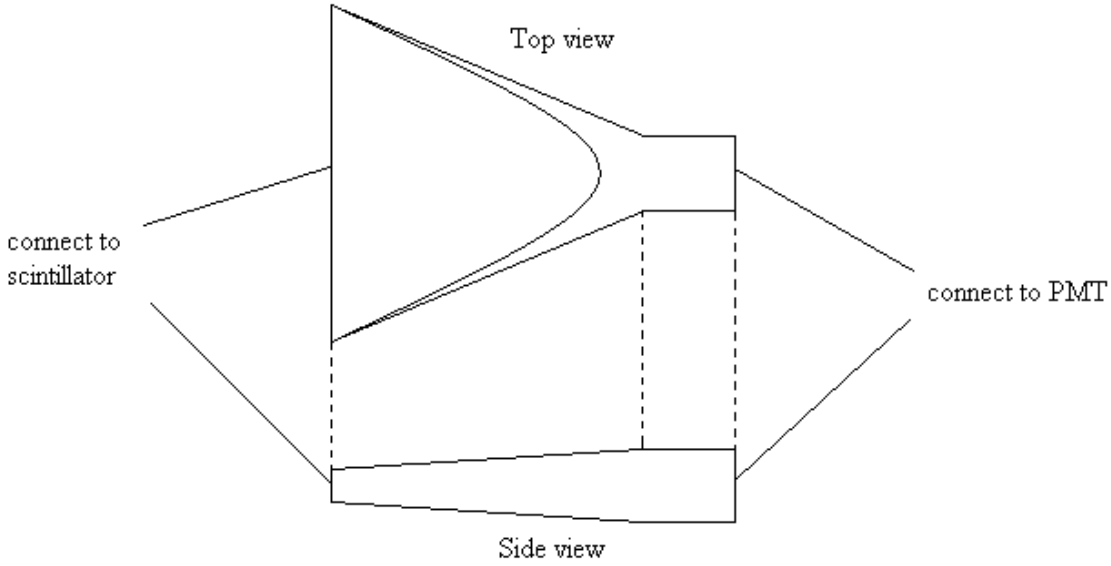

Figure 2.3: Light guide made in a form like fish tail.

The PMT we use in this experiment is BEIJING HAMAMATSU CR-105. The specifications of the PMT are listed in Table 2.1.

Table 2.1: The specifications of PMT.

Type	Head-on type
Tube Size	Dia.51 mm
Photocathode Area Size	Dia.46 mm
Wavelength (Range)	300 - 650 nm
Wavelength (Peak)	420 nm
Photocathode Material	Bialkali
Window Material	Borosilicate glass
Rise Time Typ.	7.0 ns
Transit Time Typ.	70 ns

2.2 Specifications of Electronic Device

When the particles pass the scintillation detector, it will output light and get converted in the form of electronic signal in PMT. In order to process the electronic signal, we need some electronic device. There are many kinds of specifications of electronic device using in the high energy and particle physics field, like NIM, VMEbus, CAMAC, etc. In the following section, I'll try to explain the specifications of electronic device in this experiment.

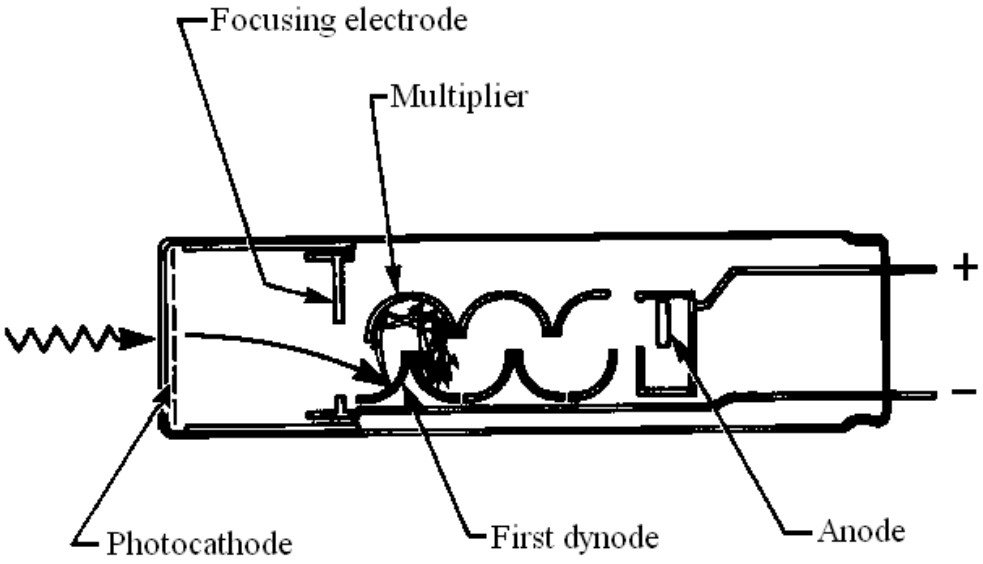

Figure 2.4: Schematic diagram of PMT.

2.2.1 NIM

NIM(Nuclear Instrument Module) is the first and simplest module designed for nuclear and high energy physics. All the NIM apparatus are designed in the form of modules according to the NIM standard mechanical and electrical specifications.

In mechanical specifications, the NIM module have a standard width of 3.43 cm and 22.225 cm height, the modules can also be designed in multiples of the standard width like double-width, triple-width, etc. All the NIM module must work on a NIM bin. The standard NIM bin is designed to accept 12 single-width modules. NIM bin supports the power for NIM module, there are six standard dc voltages are defined, $-12V$, $+12V$, $-24V$, $+24V$, $-6V$, and $+6V$.

In electrical specifications, the logic signals definition are listed in Table. 2.2. In our experiment we use the fast-negative NIM logic.

Table 2.2: The electrical specifications of NIM.

		Output must deliver	Input must accept
Slow-positive NIM logic	Logic 1	$+4V$ to $+12V$	$+3V$ to $+12V$
	Logic 0	$+1V$ to $-2V$	$+1.5V$ to $-2V$
Fast-negative NIM logic	Logic 1	$-14mA$ to $-18mA$	$-12mA$ to $-36mA$
	Logic 0	$-1mA$ to $+1mA$	$-4mA$ to $+20mA$

2.2.2 VMEbus

The VMEbus is established by Motorola, Signetics/Philips, Mostek in 1981. It derived from Motorola's "VERSAbus" which designed for the Motorola 68000 line of CPUs. VMEbus is a contracted form of Versa Module Europe bus. Here the bus is not the long car which can take many many passengers. In the field of computer, the bus means the data path on the computer that interconnects the processor with attachment devices in expansion slots.

The same as NIM the VMEbus defines a standard mechanical specifications base on the Eurocard sizes. A Eurocard is a European standard format for PCBs which uses a 96-pin plug. There are two sizes: 3U which is 10 x 16cm, 6U which is 23.335 x 16 cm for VMEbus. 3U cards support 8 and 16 bit data width and 6U cards support 32 bit data width. Each card is plugged into a backplane called VME crate. A backplane can have up to 21 slots for cards. Fig. 2.5 is the brief diagram of VMEbus crate.

Application purpose is the most difference between VMEbus and NIM system. In the NIM system, the NIM bin only support the voltage for the NIM module, there are no data transfer in the NIM bin. In the VMEbus system, the VME crate not only support the voltage for module, but also transfer data in the bus. By this feature, we can use a single board computer to control the model on VMEbus system. For example, the single board cpu is the combination of cpu, memory and mother board without pci slot, the VMEbus is the pci slot, the module is the expand card.

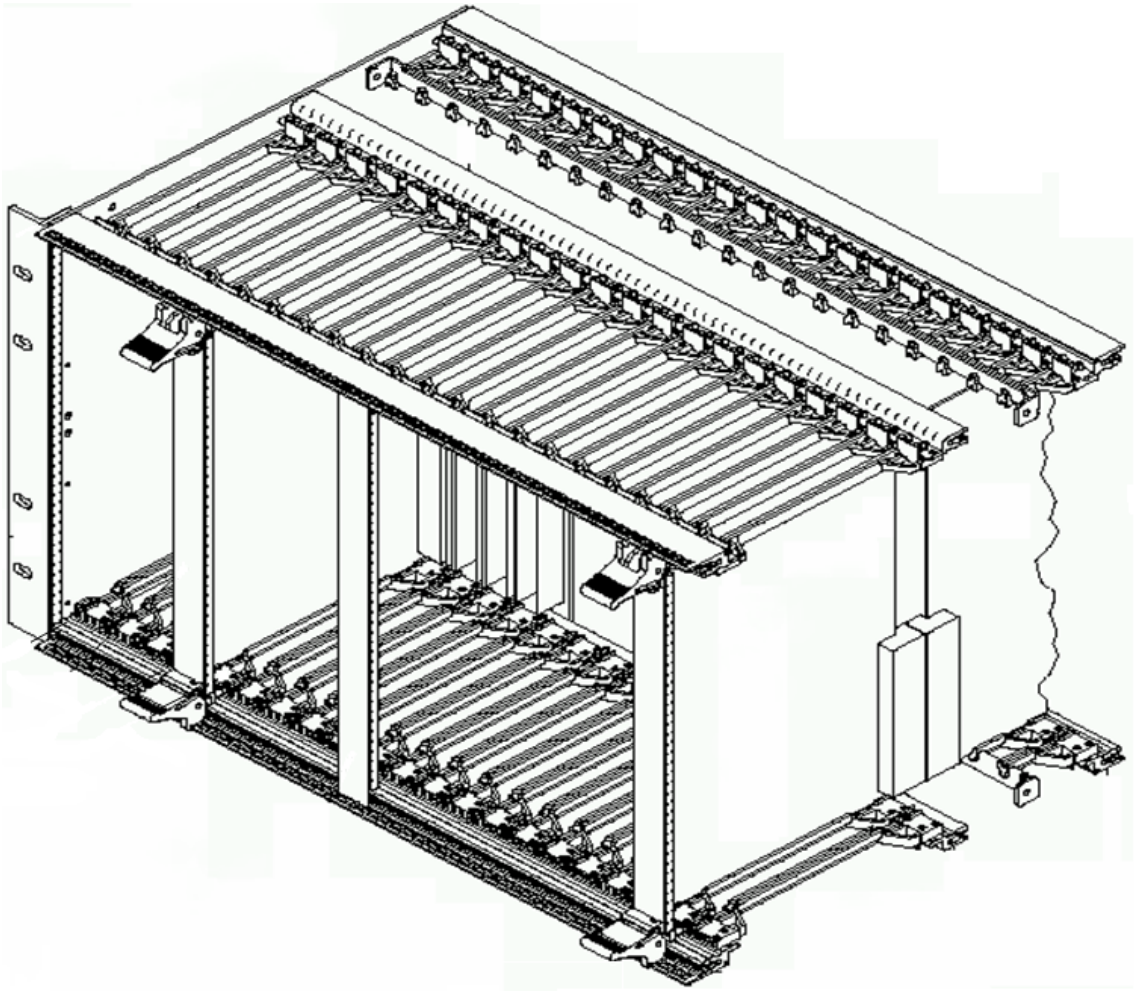

Figure 2.5: A VMEbus crate. We can simply change the module on the crate.

2.3 Electronic Device

After introducing the specifications of electronic device, in this section I will discuss the electronic device used in this experiment.

2.3.1 Discriminator

The discriminator is a device which can differentiate the analog pulse height which greater than a threshold or not. If the analog input pulse height greater than a certain threshold the discriminator responds a logic signal. If not ,it outputs no signal. The discriminator is usually used for blocking out the noise. Fig. 2.6 shows how the discriminator differentiate signal and noise. The discriminator we use in this experiment is Phillips scientific model 730 tri-mode discriminator, working in leading edge discriminator mode. The leading edge discriminator mode is a widely used mode in discriminator. The leading edge discriminator mode is that when a pulse cross the threshold level the trigger was sent immediately.

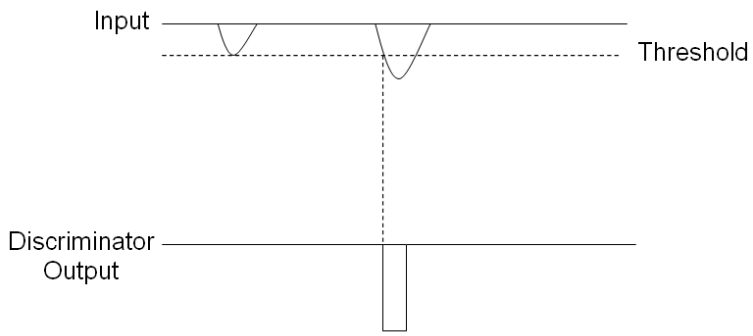

Figure 2.6: The discriminator will output a digital signal if the input pulse can surpass the threshold.

2.3.2 Linear Fan-Out

Linear Fan-out can duplicate one signal into several identical signals which have the same shape of the source signal. This is illustrated in Fig. 2.7. The fan-out come in for two kinds: linear and logic. The logic fan-out can only accept the logic signal; the linear fan-out can accept both linear and logic signal. In this experiment the linear fan-out we use is Phillips scientific model 748 octal linear fan-out.

2.3.3 Coincidence Unit

The coincidence unit can simply be imagined to be an "AND" logic gate. If there are two or more logic signals coincidence in time, the coincidence unit will output a signal. If not, it will output no signal. The Fig. 2.8 shows the operation of coincidence unit. As you can see from the diagram, the above is the event without time coincidence. There is no output from the coincidence unit. The below of the diagram is the event with time coincidence, the coincidence unit will output signal. There are two coincidence units used in this experiment, Lecroy model 365AL 4-fold logic unit, and Lecroy model 622 quad coincidence.

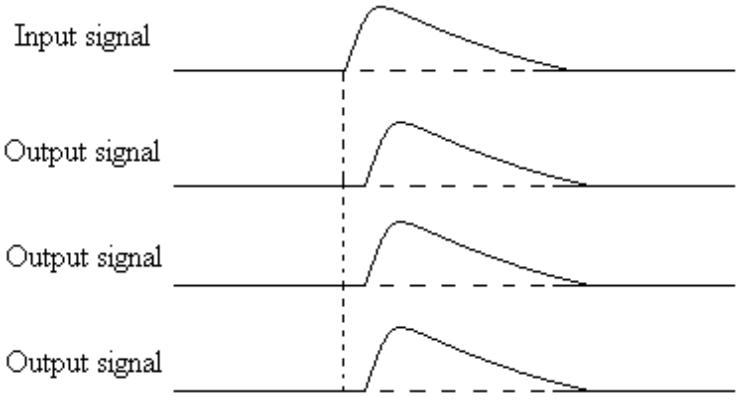

Figure 2.7: Basic operation of Linear Fan-out. Linear Fan-out module can clone the pulse.

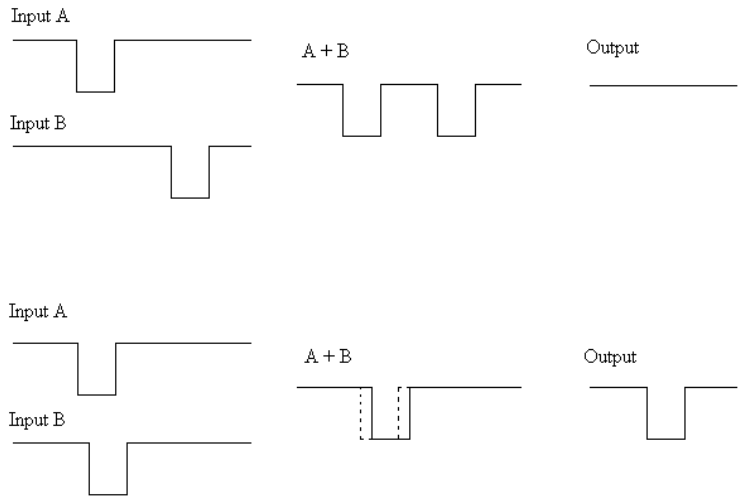

Figure 2.8: The coincidence unit operation. If the input A and B are time coincidence, the module will output a digital signal. If not, the module will output nothing.

2.3.4 Gate Generator

The gate generator is a device output a gate signal after receive a logic signal. User can adjust the gate width and delay by switching the vernier. Fig. 2.9 is an easy diagram of the gate generator operation.

2.3.5 Time to Digital Converter(TDC)

To measure a time interval in digital form, one obvious method is using an TDC. The basic principle of TDC is to start a constant frequency clock when a START signal is received. At the second STOP signal arrive, the clock will stop and give a number proportional to the time interval between the START pulse and STOP pulse.

Fig. 2.10 shows the basic principle of TDC. When a start signal input to the TDC the clock is running, after stop signal arrive the clock then stop and deliver a time interval about the start signal and stop signal.

The TDC module we used is LeCroy model 1176 16 channel VME TDC module, which was operated in the common stop mode. The specifications of the TDC module is list in table 2.3.

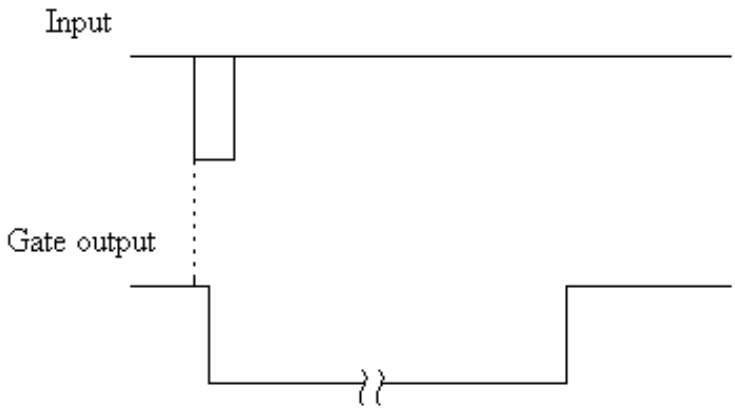

Figure 2.9: The gate generator operation. When the gate generator received a signal, it will output a gate.

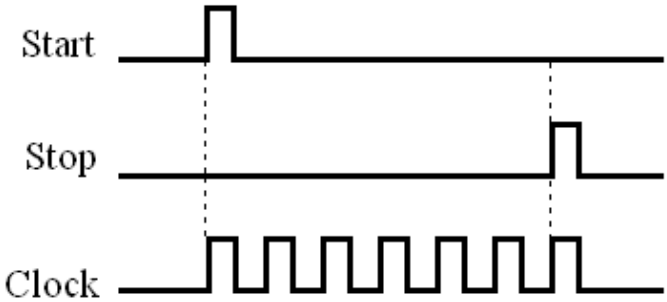

Figure 2.10: Working principle of the TDC. When the TDC received a start signal the internal clock will start count, until the TDC received a stop signal and the TDC will output the clock counts.

2.3.6 Analog to Digital Converter(ADC)

The ADC is a kind of fundamental link between analog signal to digital electronics. ADC converts the analog signal's information to an equivalent digital form. Fig. 2.11 shows a method named Wilkinson method. First, the input pulse is used to charge a capacitor. When it ends, the capacitor then "run down". At the start of the "run down", the clock in a constant frequency is turned on. After discharge complete, the clock stop. The number of clocking is proportional to the height and strength of the input pulse.

The ADC module we used is LeCroy model 1182 VME multiple channel input charge ADC module. The specifications of the ADC module is listed in Table. 2.4.

There are generally two kinds of ADC, charge-sensitive ADC, and peak-sensitive ADC. One example of charge-sensitive ADC is the ADC built up by Wilkinson method introduced in above. The measurement result of charge-sensitive ADC will depend on the total charge of

Table 2.3: The specifications of LeCroy 1176 TDC.

Channel	16
Full scale	65.556 μsec
Range	16 bits
Multi-event Buffer	32
double pulse resolution	40 $n$sec
Least Significant Bit	1 $n$sec

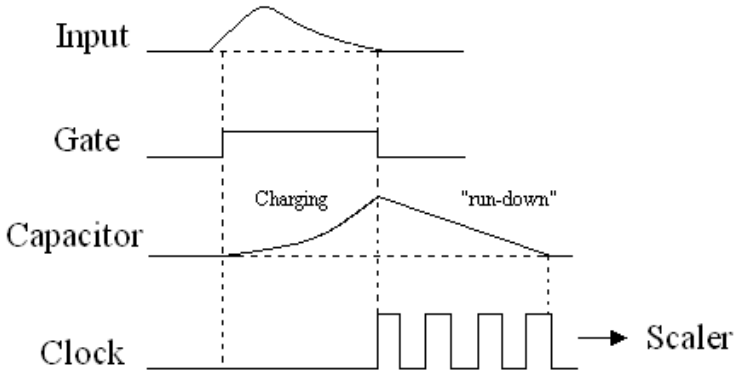

Figure 2.11: Wilkinson method of ADC. The capacitor will start charging when the ADC received a gate. When the gate disappear the capacitor will start discharge and a clock will start running at the same time. When the discharge was done the lock will output it's counts, the counts can tell us the charge information of the input pulse.

the input pulse. But the peak-sensitive ADC is not. It is only sensitive to the pulse height. The measurement of peak-sensitive ADC will depend on the height of the input pulse. In this experiment we use the charge-sensitive ADC.

Table 2.4: The specifications of LeCroy 1182 ADC.

Channel	8
Fullscale	65.556 μsec
Range	12 bits(dynamic)
Multi-event Buffer	16
Sensitivity	50 fC/count

Chapter 3

Basic Definition and Experiment Setup

The basic definition used in this experiment will be introduced. The experiment setup like gate condition and DAQ system will be also introduced.

3.1 Basic Definition

In this section, I would like to outline the basic definition of muon lifetime and muon capture.

3.1.1 Muon Lifetime

The muon is a typical process of radioactive decay. The radioactive decay is a random process, independent of the previous life of the particle.

Suppose at time t we have $N(t)$ muons, then the decay rate is $\frac{-dN}{dt}$. The decay rate is proportional to N. The relation of decay rate and the numbers of muon is:

$$\frac{-dN}{dt} = \lambda N \tag{3.1}$$

The λ is a constant "decay constant." We can transposition the equation (3.1) and have:

$$\frac{1}{N} dN = -\lambda dt \tag{3.2}$$

After integrating equation(3.2), we will have:

$$\ln N = -\lambda t + C \tag{3.3}$$

Here the constant C is integrating constant. The equation(3.3) can change to:

$$N(t) = N_0 e^{-\lambda t} \tag{3.4}$$

The N_0 is the number of muons at $t = 0$. The truth is that the number of muons exponentially decreasing.

When we say "muon lifetime" it often means the mean lifetime of the muon. The mean lifetime τ is the inverse of decay constant $\tau = 1/\lambda$.

But there are still a question. We can not prepare a pool of muons and can not measure all the lifetime. It is fortunate that the radioactive decay is exponentially distributed. We can measure the lifetime of the muons which enter our detector at random times. The lifetime and the number of muons are still in the exponential form of the radioactive decay. For example, we can drafting a figure, the y-axis is the number of muon and the x-axis is the lifetime of the muon. By obtaining a logarithmic scale on the y-axis and fitting the curve by

$y = C_{free}e^{-t/\tau_{free}} + C_{pedestal}$ we can get the mean lifetime τ_{free}. Here t is time, y is the counts number, C_{free} is the constant correlate with the muon decay event number, τ_{free} is the mean lifetime, $C_{pedestal}$ is the pedestal which produced by the random accidental coincidence noise. We suppose the noise is random occur in any time. The noise will increase the counts. So, we add a constant of pedestal to remove the effect produced by noise.

3.1.2 Muon Capture

The effect of muon capture will vary the result of muon lifetime measurement.

Let us look at the muon capture process $\mu^- + p \rightarrow n + \nu_\mu$, there are no charged particles after processing, the neutron and muon neutrino have zero charge. According to the principle of the scintillation detector, it should not output any signal. Fortunately, the capture process will produce a neutron, we can use the plastic scintillator to detect the neutron.

In order to detect the neutron, the most common method is using another charged particles to replace the kinetic energy of the neutron. The plastic scintillator or organic scintillator contain large amounts of hydrogenous material. The neutron in the plastic scintillator or organic scintillator may have a strong probability to collide with the hydrogen's proton and transfer kinetic energy to the proton. The proton collided by neutron may get enough energy to excite the scintillation material then the scintillator will output some photon.

Because of the relative short lifetime of capture process, the lifetime we measured will less than free decay lifetime. The math form of free decay lifetime we discussed above was $y = C_{free}e^{-t/\tau_{free}} + C_{pedestal}$. The capture decay lifetime have the same form. The lifetime contain free decay and capture decay can be rewrote to:

$$y = C_{free}e^{-t/\tau_{free}} + C_{cap.}e^{-t/\tau_{cap.}} + C_{pedestal} \tag{3.5}$$

Here the t is time, y is the counts number, C_{free} and $C_{cap.}$ are constants correlate with the muon decay event and capture decay event, τ_{free} is the mean lifetime of free decay, $\tau_{cap.}$ is the mean lifetime of capture decay, $C_{pedestal}$ is the random accidental coincidence which produced by the noise.

3.2 Experiment Setup

The experiment setup will be discussed in this section. The DAQ system will also be discussed in this section.

3.2.1 The Flow Path of Experiment

Fig. 3.1 is the flow path of this experiment. When the physics events occur, the detector will collect the signal and send it to the electronic device. After the electronic device receive the signal, the electronic device will determine the signal which is noise or real physics event, and transform the real physics event signal in digital form. The digital form signal will be transferred to the DAQ system. Here, "DAQ" is the abbreviation of "data acquisition". The DAQ system will save the information of the signal in "RAW data" form to the data storage system. The above I listed are completed just after the physics events occur, so we often call it "online analysis".

After online analysis, the RAW data were save in the data storage system. We can rewrite the RAW data to a file format "Ntuple" and analyze it by a software "PAW"[11]. After the analysis, we can get the physics results. Because the data analysis are not an online process, we often call the analysis process "offline analysis".

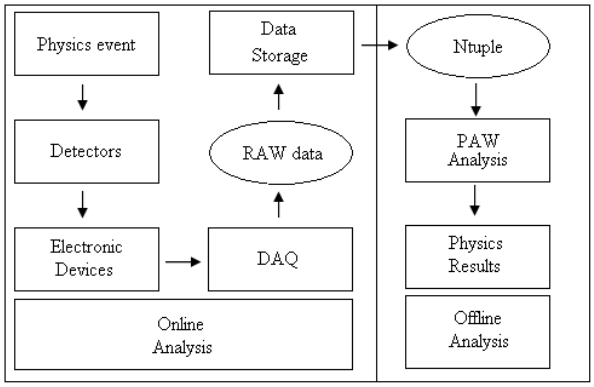

Figure 3.1: The flow path of experiment.

3.2.2 Experiment Setup

Fig. 3.2 shows the block diagram of total experiment setup. I will discuss it in three parts, detector, NIM modules, and VME modules.

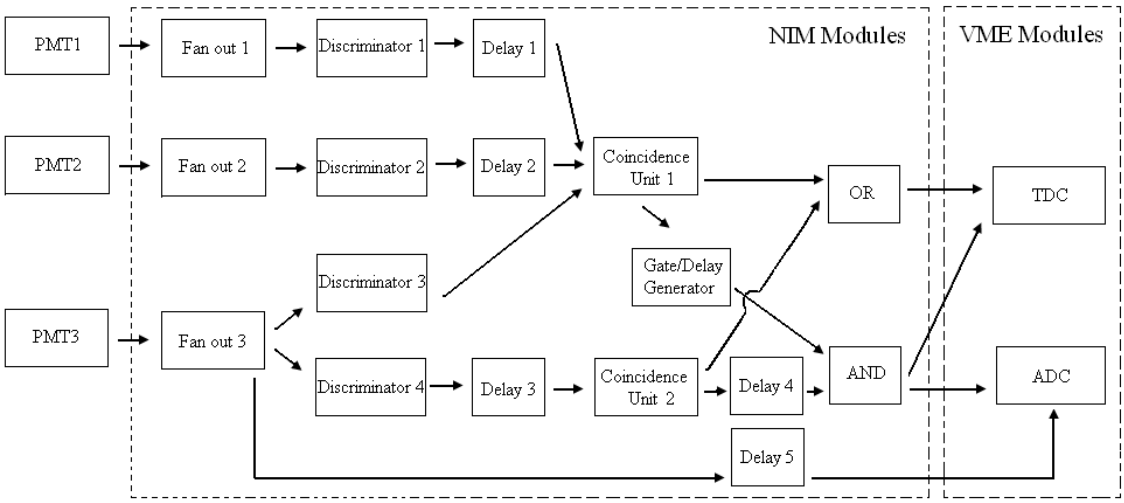

Figure 3.2: Block diagram of experiment setup.

Detector

As we can see from the Fig. 3.3, it shows the basic structure of the detector used in this experiment. The detector contains three layers of scintillation detector and one layer of target metal which placed at the middle of the layer 2 and layer 3 scintillator. When the cosmic muon passing through the detector, the muon which have specific energy may cross the layer 1 and layer 2 scintillator but stop in the target layer. When the muon stop in the target layer it may be captured by the target nuclei. After the capture process, one neutron will be released. If the neutron just right reach to the layer 3 scintillator, and just right transmit its energy to the scintillator's proton, the scintillator can output some signal to the electronic device. The neutron produced by capture process may reach to layer2 and layer1 scintillator. But, we do not collect this kind of signals.

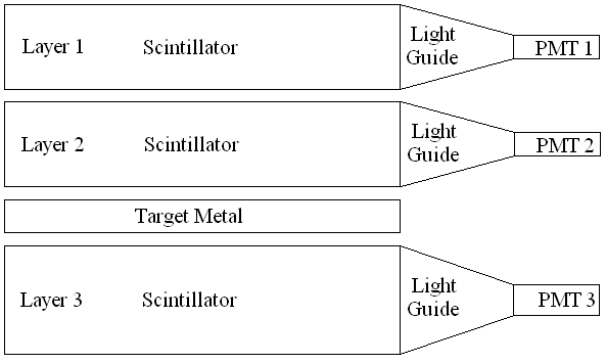

Figure 3.3: Structure of detector. In this experiment we use three scintillation detector and a layer of target.

NIM Modules

The most important thing for the NIM module in this experiment is to determine the signal from the PMT which are real physics events or not. We suppose that the muon comes from the top atmosphere, incidents to our detector, stop in the target and then captured by the target nuclei. Basic on this expect, the muon will trigger the layer 1 and layer 2 scintillator first, at the same time. After a very short moment, the layer 3 scintillator will be triggered.

The Fig. 3.4 is the timing chart of the NIM modules. When a muon pass through the layer 1 and layer 2 scintillator, those two scintillator will output some photons and the photons will be collected by the PMT 1 and PMT 2. The PMT 1, 2 will output the signals to the fan out modules first, and the fan out modules will duplicate one signal into several identical signals. The fan out modules will send the signal to discriminator 1 and discriminator 2, and discriminator 1, 2 will output the signal in digital form. If the muon just stopped right in the target layer, the PMT 3 will collect no signal then the discriminator 3 will output no signal. The coincidence unit 1 is set to be triggered under the conditions of discriminator 1, 2 were triggered, but discriminator 3 was not. If the conditions were fitted, the coincidence unit 1 will output a signal. The signal output by the coincidence unit 1 will trigger two modules the gate/delay generator and a "OR" logic gate. After triggered by the coincidence unit 1 the gate/delay generator will output a $10\mu sec$ gate, and the "OR" logic gate will output a signal, too.

Several nano-seconds later, the proton produced by capture process or the electron produces by muon free decay is reach to the layer 3 scintillator, and detected by the PMT 3. The PMT 3 will output to the fan out module first. Then three signals will be output from the fan out module, one of the signals is sent to discriminator 3, another one is sent to discriminator 4, the other one is sent to delay 5. The discriminator 4 will send the digital signal to delay 3 which delay the same time as delay 1, 2. After through the delay 3 module, in order to fit the delay time with the signal from coincidence unit 1, the signal from delay 3 will also be sent to coincidence unit 2. The coincidence unit 2 will send out two signals. One of the signals is sent to the "OR" logic gate, and the other one is sent to delay 4.

If the muon passing through the layer 1, 2 scintillator, captured by target nuclei or free decay in the target layer, and the proton or electron just arrived right the layer 3 scintillator, the "OR" logic gate will send two signals which contain the timing information of the incoming muon and decay or capture process occurred. After a few nano-seconds the "AND" logic gate will also send a signal which for stop the TDC and gating the ADC, these details will be discussed later. And the delay 5 module will send a pulse contain the charge information of the capture or decay process produced particle to the ADC.

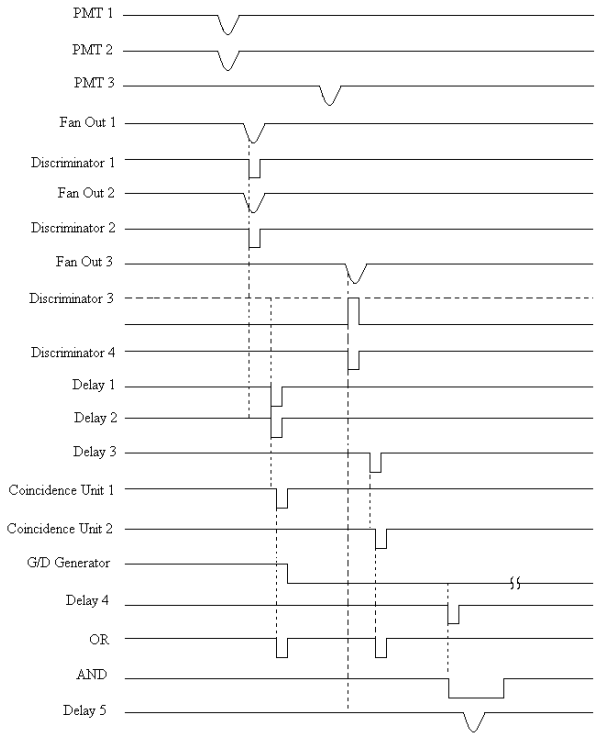

Figure 3.4: Timing chart of the NIM modules.

VME Modules

In this experiment we use two VME modules, ADC and TDC. To control the modules, we must send some signals to trigger them. In order to trigger the ADC module, we must send a gate which have width between $50nsec$ to $2\mu sec$. Look back on the Fig. 3.2 and Fig. 3.4, we can see the "AND" logic unit sends a gate to ADC, and the delay 5 just delay the signal on the gate's time range and sends the signal to ADC. Because of some internal component delay, the ADC module will work after $25nsec$ the gate input, and save the pulse charge information. Fig. 3.5(a) is the ADC general operation flowchart.

After setting the ADC, the ADC is waiting for the gate coming. When the gate coming, the ADC will save the pulse charge information until the gate end or some outer clear signal input. After data acquisition, the ADC will quickly save the data to its memory and waiting for next event.

The TDC module used in this experiment can operate in two kinds of modes, "common start" and "common stop". The "common start" means the TDC starts working when a start signal was input, and will stop after a short span which defined by user. "Common stop" means the TDC will work after any signal input and will stop after the stop signal income. If the signal input but without any stop signal input, the TDC will not save this data, and will wait for the next event. In this experiment, because of the gate condition, we choose to use the common stop mode. Fig. 3.5(b) is the TDC operation flowchart in common stop mode. From the flowchart, we can see that, after setup, the TDC is waiting for the event coming. After event coming, the TDC will wait for the common stop coming. If it comes, the TDC will stop and saving the data and wait for next event.

3.2.3 Data Acquisition(DAQ) System

FIG. 3.6 shows the global structure of the DAQ system. We can see that the ADC and the TDC is controlled by single board computer on VME bus. When we insert VME modules into

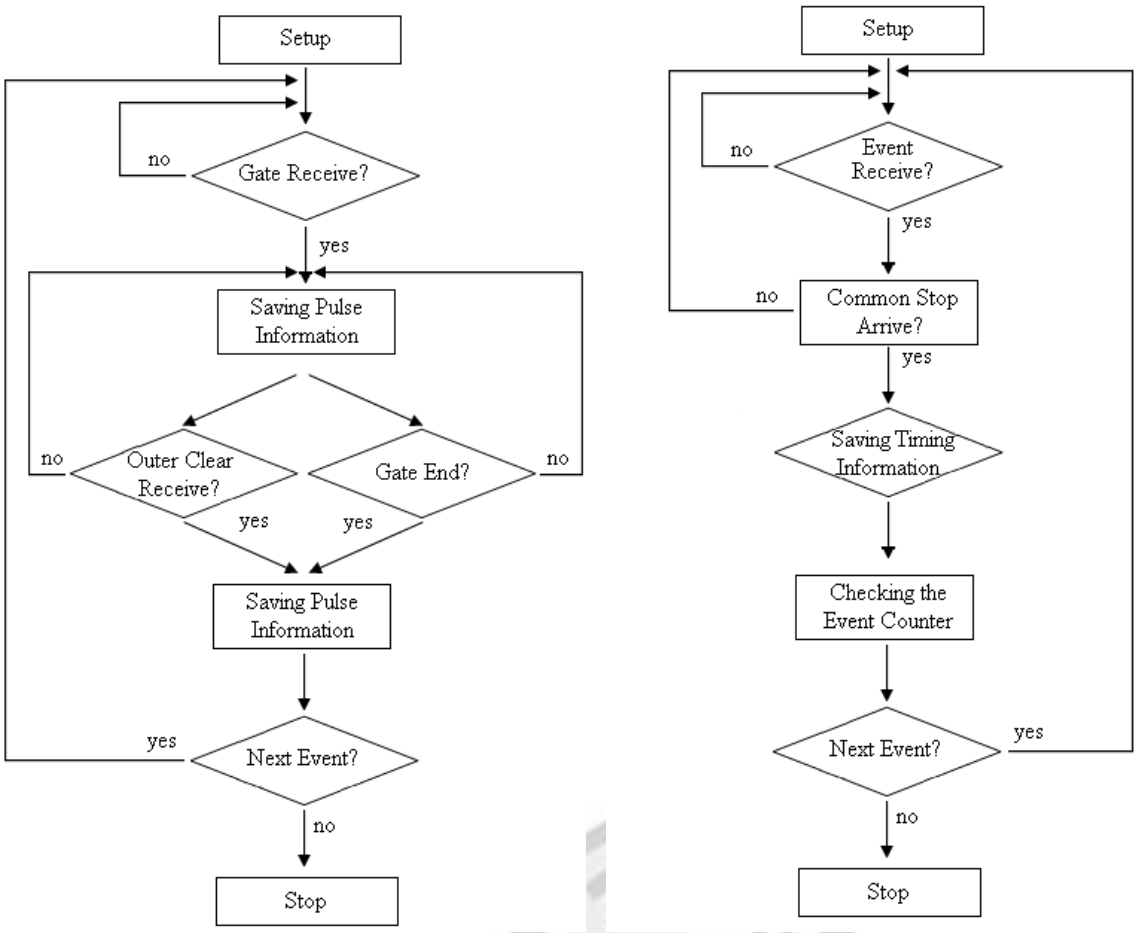

(a) ADC general operation flowchart. (b) TDC flowchart.

Figure 3.5: ADC and TDC flowchart.

the VME crate we must setup the module's base address first. After inserted, the single board computer will mirror some of its memory to VME module's memory. We can operate modules and read the data by carefully operate the single board computer's memory.

The single board computer is connecting with a SCSI hard disc and using "Solaris 8" Operating system. All the data produced in this experiment will save in "RAW" data form in the SCSI hard disc first. The single board computer can connect to ethernet, too. So, we can use any desktop computer connecting to the single board computer and get the data to analyze.

3.3 Calibration of the Experiment Apparatus

In this section, the calibration of PMT working voltage and the efficiency of electronic apparatus in different time scale will be introduced.

3.3.1 Calibration of PMT working voltage

The counting efficiency of PMT depends on the working voltage of the PMT. In order to find the suitable working voltage, we must make a so-called plateau measurement. Generally speaking, the working voltage and the counting efficiency are linearly increasing before the plateau region, and in the plateau region, the counting efficiency is not increase outstanding with the increase of working voltage. When the working voltage is over the plateau region, the PMT is work in

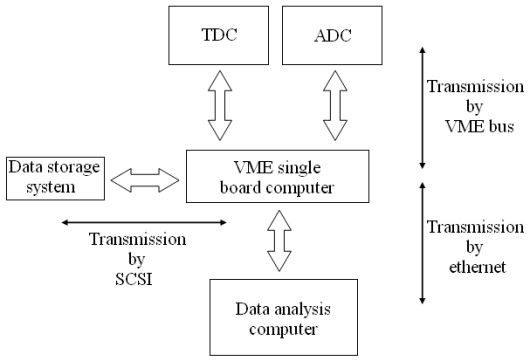

Figure 3.6: The structure of DAQ system.

a nonlinear region, the counting efficiency is increase very fast with working voltage increasing. FIG. 3.7 shows the diagram of plateau.

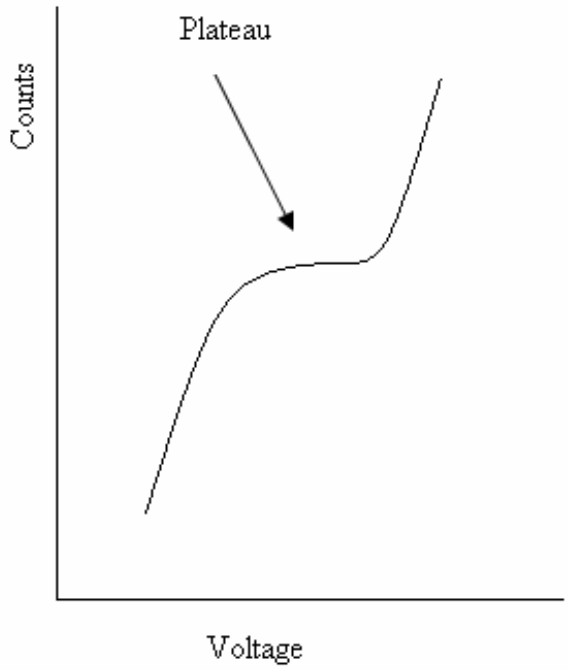

Figure 3.7: The diagram of plateau. In this experiment the suitable PMT working voltage is in plateau region.

The measurement setup is shown in FIG. 3.8. First, connect the detector to the discriminator. Second, use a counter to count the counting rate. Finally, plot a diagram with the counting rate VS. working voltage. The counter is controlled by a Visual Basic(VB) program. We will discuss the VB program in Appendix. A. The measurement results are diagrammed in FIG. 3.10. After finish this plateau measurement, we found that we can not determine the plateau region for PMT 1, and PMT 2, there are no plateau in FIG. 3.10(a) and FIG. 3.10(b).

In order to find a suitable working voltage for PMT 1 and PMT 2, we must make a coincidence plateau measurement. Coincidence plateau measurement is to use a trustable PMT and working in the plateau region, coincidence with the test PMT and measuring the counting rate. FIG. 3.9 shows the setup of coincidence plateau measurement. The test detector's counting rate is constrained by the reference detector, the counting rate will finally reach a fixed number. The plateau region is near the working voltage when the counting rate is starting to

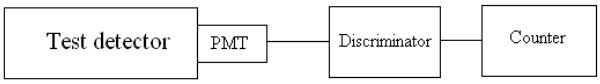

Figure 3.8: Plateau measurement setup.

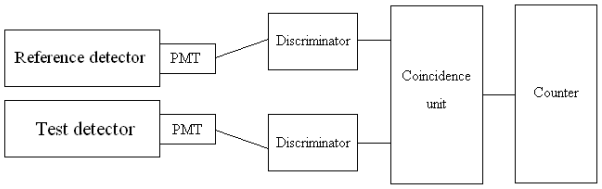

Figure 3.9: Coincidence plateau measurement setup.

be fixed. FIG. 3.11 displays the coincidence plateau measurement results. From FIG. 3.11(a), FIG. 3.11(b), and FIG. 3.10(c) we choose the working voltage and threshold of the discriminator for PMT 1, 2, 3 are listed in Table. 3.1.

Table 3.1: The working voltage and threshold voltage for detectors.

PMT	Working voltage	Threshold voltage for discriminator
1	-1050V	-200mV
2	-1000V	-100mV
3	-950V	-100mV

3.3.2 Calibration of the Efficiency of Electronic Apparatus in Different Time Scale

The electronic apparatus may have different data acquisition rate in different time scale. In order to consider this effect, we must calibrate the efficiency of electronic apparatus in different time Scale. This test using a gate/delay generator to replace the three PMT. The setup is like FIG. 3.12. We use the gate/delay generator to produce two pulse. The first pulse is transferred to the fan out 1 and fan out 2. After several nano-sec later, the second pulse is transferred to the fan out 3. We can adjust the delay between first pulse and second pulse to measure the acquisition rate in different time scale. Finally, there will output two signal in the "OR" logic gate and will output one signal in the "AND" logic gate. We connect the "OR" and "AND" logic gate to a counter in different channel, the counter will output the counting results. The ratio of the two counting should be 2:1, if not, we must try to correct the counting rate in different time scale. After measuring many times, the ratio of the two counting are all 2:1. We don't need to correct the counting rate in different time scale.

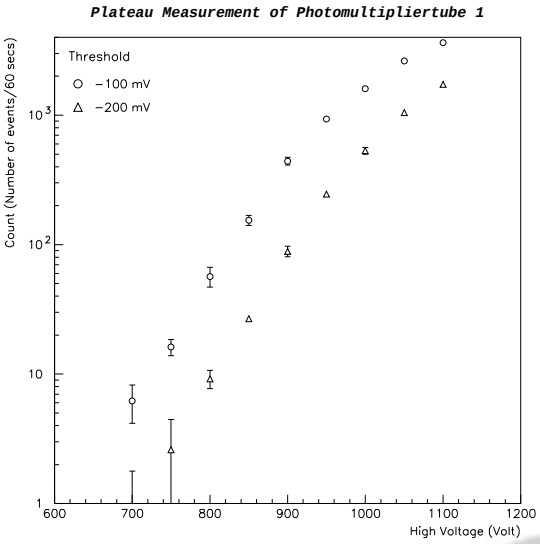

(a) Plateau measurement results of PMT 1.

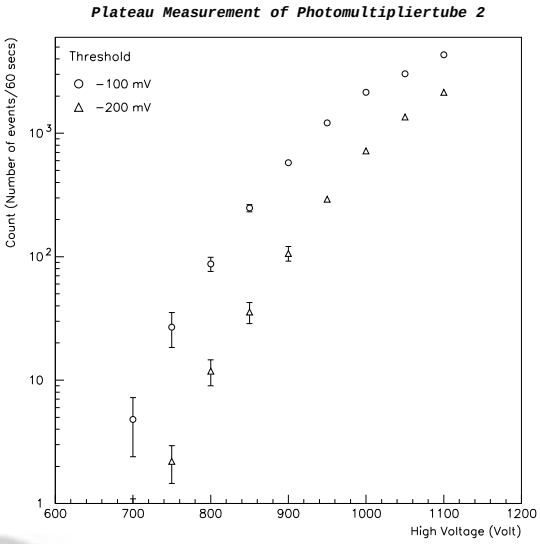

(b) Plateau measurement results of PMT 2.

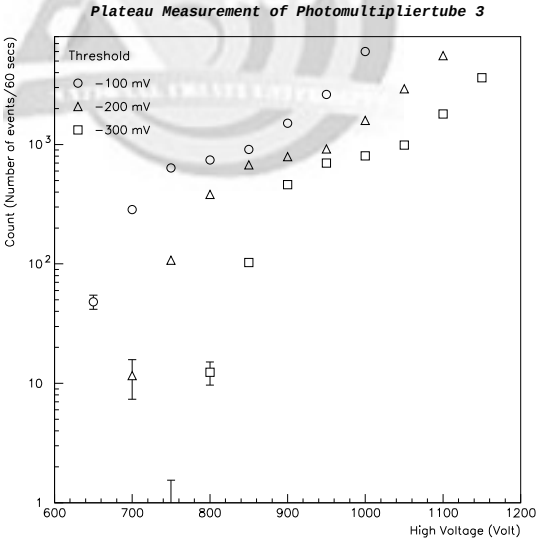

(c) Plateau measurement results of PMT 3.

Figure 3.10: The plateau measurement results. In (a) and (b) we can not clearly find out the plateau region and in (c) the plateau region is very obvious.

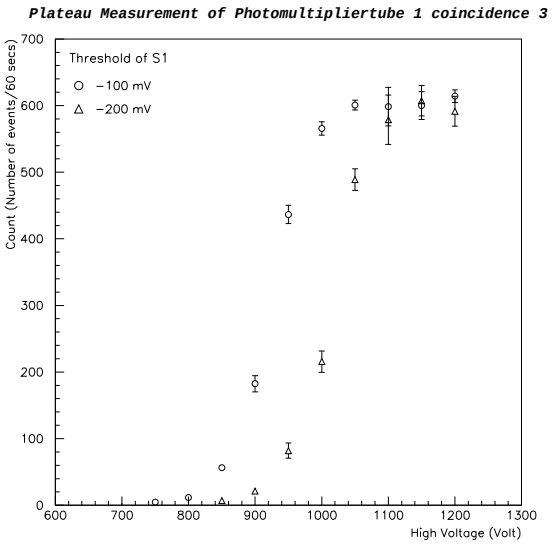

(a) Plateau measurement results of PMT 1 coincidence with PMT 3.

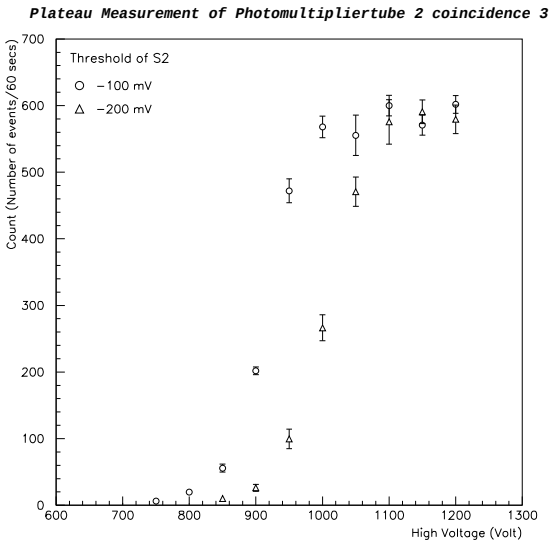

(b) Plateau measurement results of PMT 2 coincidence with PMT 3.

Figure 3.11: The coincidence plateau measurement results. The counts is constrained by coincidence with PMT3, and we choose the first several point to be the plateau region.

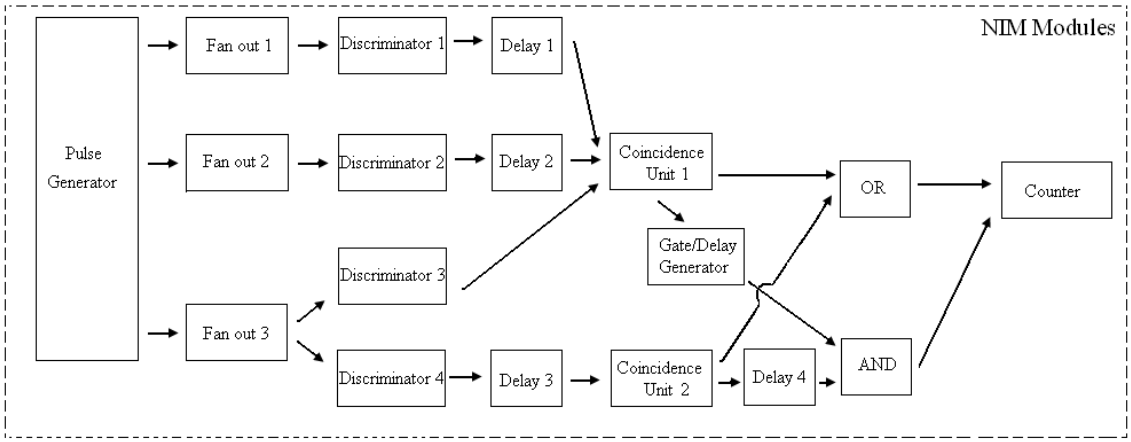

Figure 3.12: The setup of testing the efficiency of electronic apparatus.

Chapter 4

Data Analysis and Results Discussion

4.1 Data Analysis Procedure

In this section the data analysis procedure of TDC and ADC data are presented. Both TDC and ADC data are analyzed by PAW.

In this experiment we use three kinds of metal to be the target and try to measure the muon captured lifetime by the metal nuclei. Finally, we compare the fitting result with the Z^4 dependence. Besides the measurement of these three targets, measurement using the same set up without any target is also done, we called "BG" afterward in the purpose of understanding the influence of electronic noises and systematic error.

4.1.1 TDC Data Analysis Procedure

In this experiment we use the Time to Digital Converter(TDC) to measure the pulse's timing information and try to fit the lifetime of free decay and captured decay.

As discussed in section. 3.2.1, we use PAW to analyze the RAW data which was saved in a file format "Ntuple". After using PAW to read the Ntuple, we merge the data into many bins. The bins have two kinds of scale. From the discussion in section 3.1.2, we suppose the capture events appear in the front side of time scale. We merge the data in two different time scale, FIG. 4.1 shows the situation. The first part is the data merge in small time scale; the last part is merged in big time scale. From the section. 3.1.2 it can be seen that the muon capture process can be described by $y = C_{free}e^{-t/\tau_{free}} + C_{cap.}e^{-t/\tau_{cap.}} + C_{pedestal}$. To Compare with the FIG. 4.1, because the $\tau_{cap.}$ is much less than τ_{free}, we assume the last part in the figure can only influence the C_{free}, $C_{pedestal}$ and τ_{free}, we also call this part "free decay part". The first part can influence the C_{free}, $C_{cap.}$, τ_{free}, $C_{pedestal}$, and$\tau_{cap.}$. So, we can fit the free decay part first to decide the C_{free} and τ_{free}. After decide the C_{free} and τ_{free}, we can fit whole part to decide the C_{free},$C_{pedestal}$, and $\tau_{cap.}$.

In order to decide the C_{free} and τ_{free} first, we must to find the suitable fitting start point and end point of free decay part.

The flow path of TDC data analysis decided by us are: First, fix the start point in $0ns$ and change the end point to find the stable result. Second, fix the end point measured in first step, and change the start point to find stable result. Third, fit the free decay part which between the end point and start point to decide C_{free}, $C_{pedestal}$, and τ_{free}. Fourth, fit total part to decide $C_{cap.}$, $C_{pedestal}$, and $\tau_{cap.}$.

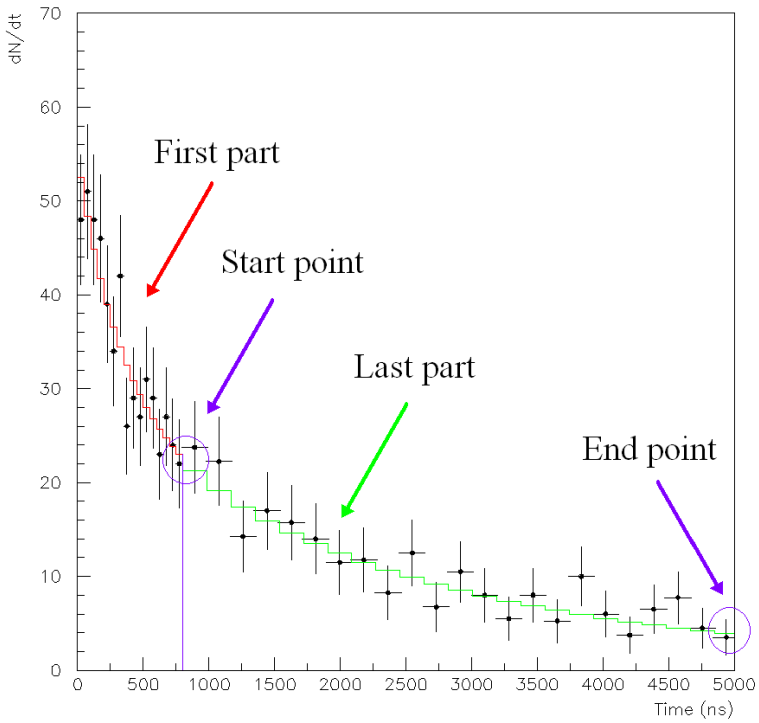

Figure 4.1: The different vector size in TDC data. The first several bins are cut in a small scale and after it are cut in bigger scale.

4.1.2 ADC Data Analysis Procedure

In this experiment we want to use the ADC to measure the pulse's charge information and try to differentiate the free decay events and capture decay events by the information from ADC. The ADC analysis procedure we use in this experiment are: First, analyze the ADC VS. TDC profile. Second, compare the probability of compatibility between two ADC distribution. Third, we make different ADC cut and analyze the TDC data for each ADC cut.

4.2 Monte Carlo Simulation

Monte Carlo simulation is computer simulation to reconstruct the physics events. The monte carlo simulation we use in this experiment is based on C language. The complete program code is listed in Appendix B. In this experiment, in order to confirm the accuracy of our analysis code, we use Monte Carlo method to generate a huge amount of fake events for muon free decay and muon captured decay data. The data generated by Monte Carlo method have the same form like the raw data generated by the DAQ system. We can use our analysis code to analyze this data. Because we can adjust the data by changing the constant in the Monte Carlo code, we can test the correctness of analysis code.

We generate the muon free decay data by using a log distribution function. The function is:

$$Y = \tau_{free} \times log(\frac{X}{C_1}) \tag{4.1}$$

Here C_1 is a constant, τ_{free} is muon lifetime, X is a random number, Y is the output data.

The muon captured decay data is generated by the Eq. (4.1) and plus another part:

$$Y = \tau_{cap.} \times log(\frac{X}{C_2}) \tag{4.2}$$

Here $\tau_{cap.}$ is muon capture lifetime for specific atom, C_2 is a constant. We set the τ_{free} is 2197 and $\tau_{cap.}$ is 164.

Because we don't have any theoretical speculation about the ADC distribution, in this experiment we only use the Monte Carlo simulation to test the TDC analysis code.

4.2.1 Monte Carlo Simulation Result

We use the data generated by Monte Carlo simulation to confirm the accuracy of our analysis code. The result is presented in FIG. 4.2 to FIG. 4.4(b).

FIG. 4.2 shows the results of changing the data's fitting end point for free decay part. The results of this measurement can help us to find the suitable end point for free decay part which we already discussed in section. 4.1.1. The red dotted line shows the world average free decay lifetime. We can find that from FIG. 4.2(b) the fitting results have a trend to be smooth in the last several points. So, we decide to use all data, and choose $10000ns$ to be the end point of free decay part.

Looking at the FIG. 4.2(a), it has different situation with FIG. 4.2(b), the fitting results are stable in the last several point swiftly. We choose $10000ns$ to be the end point. The $10000ns$ is the limit set by us of the TDC acquisition time range, too.

Comparing the FIG. 4.2(a) and FIG. 4.2(b), we can find in FIG. 4.2(b) all the value is less than the world average. It's because all the fitting start point is in $0ns$, the fitting contains the capture decay event. Because the capture decay event will increase the counts in the first several bins. This effect will increase the slope. The lifetime will be less than world average.

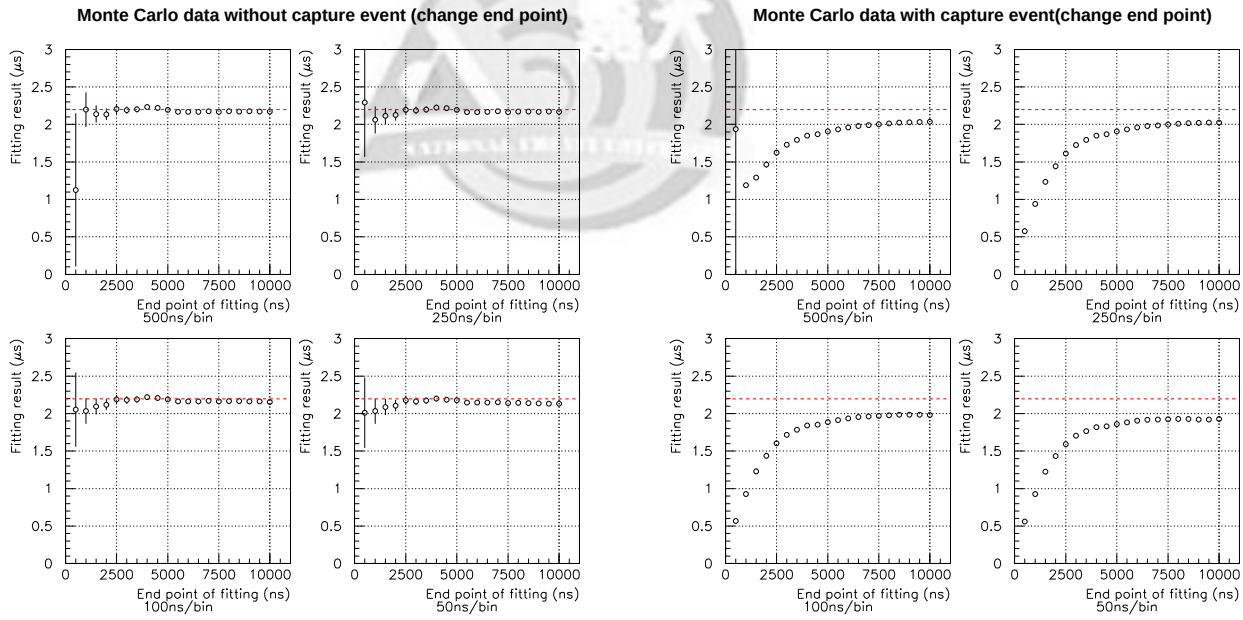

(a) The result of changing the Monte Carlo data without capture event fitting end point.

(b) The result of changing the Monte Carlo data with capture event fitting end point.

Figure 4.2: Changing end point for free decay. Because the captured events adding in (b), the fitting result have a difference trend between (a) and (b).

From FIG. 4.3, we can see the result of change the start point for free decay part. This analysis can help us to decide the start point of free decay part. After decide the start and end point of free decay part, we can fit the free decay part to decide the C_{free} and τ_{free}.

FIG. 4.3(a) are the results of changing the Monte Carlo data without capture event fitting start point. FIG. 4.3(b) are the results of changing the Monte Carlo data with capture event

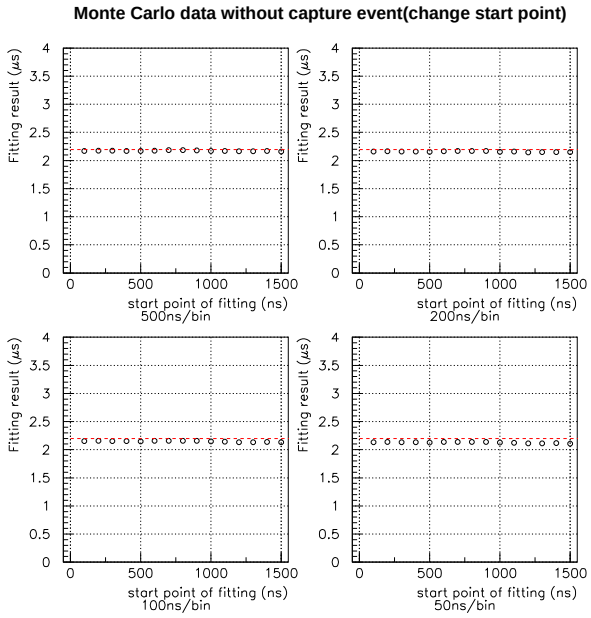

(a) The result of changing the Monte Carlo data without capture event fitting start point.

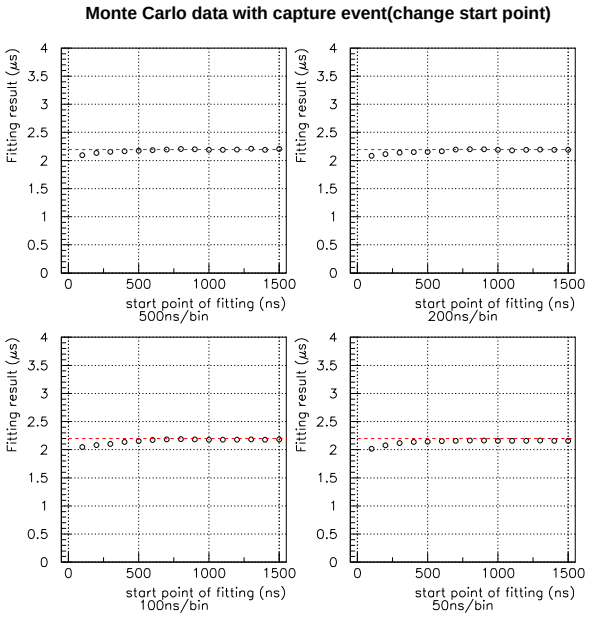

(b) The result of changing the Monte Carlo data with capture event fitting start point.

Figure 4.3: Changing start point for free decay. The fitting result in (a) are all the same, but in (b), because the captured events adding the first several points have different fitting result.

fitting start point. Comparing FIG. 4.3(a) and FIG. 4.3(b). The first three point of FIG. 4.3(b) are lower than the first three point of FIG. 4.3(a). This situation is come from the captured decay events we discussed in the FIG. 4.2(b). The captured decay muon events will increase the counts of first several bins. If we fit the data contained the captured decay muon events, the result of fitting will have a lower value. We can use this analysis to find out the range which influenced by the muon captured events, and do not fitting the range to have a pure free decay part.

From FIG. 4.3(b) we can find that the trend of lifetime after $600ns$ are almost gradual. We choose the $600ns$ point to be the fitting start point. The FIG. 4.3(a) have no captured muon events, we can see that the fitting results are all the same, no matter how we change the start point.

FIG. 4.4 are the results of fitting the Monte Carlo simulation data. FIG. 4.4(b) is the result of fitting with capture decay events. The free decay lifetime is $2.169 \pm 0.065\mu s$, the capture decay lifetime is $0.175 \pm 0.018\mu s$. The value of free decay lifetime and captured decay lifetime set by us in Monte Carlo simulation is $2.197\mu s$, and $0.164\mu s$. Within error bar the fitting result of free decay lifetime and captured decay lifetime are consistant with our set.

FIG. 4.4(a) is the result of fitting without capture decay events. The free decay lifetime is $2.167 \pm 0.031\mu s$, the capture decay lifetime is $0.447 \pm 0.245\mu s$. This data is produced by Monte Carlo method and we don't include the capture event in this data. We can find that the lifetime is less than world average, and a capture decay lifetime was occur. This situation may occur because we use the function $y = C_{free}e^{-t/\tau_{free}} + C_{cap.}e^{-t/\tau_{cap.}} + C_{pedestal}$ to fit the data. FIG. 4.4(c) shows the data fitted by $y = C_{free}e^{-t/\tau_{free}} + C_{pedestal}$. The free decay lifetime $2.181 \pm 0.030\mu s$is more close to the value $2.197\mu s$ we set.

The fitting results are close to the value we set. We can trust our analysis code.

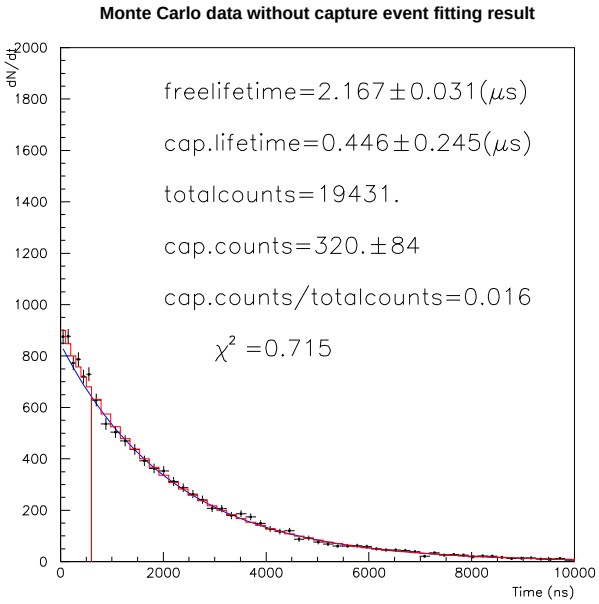

(a) Result of Monte Carlo simulation data without capture event fitting.

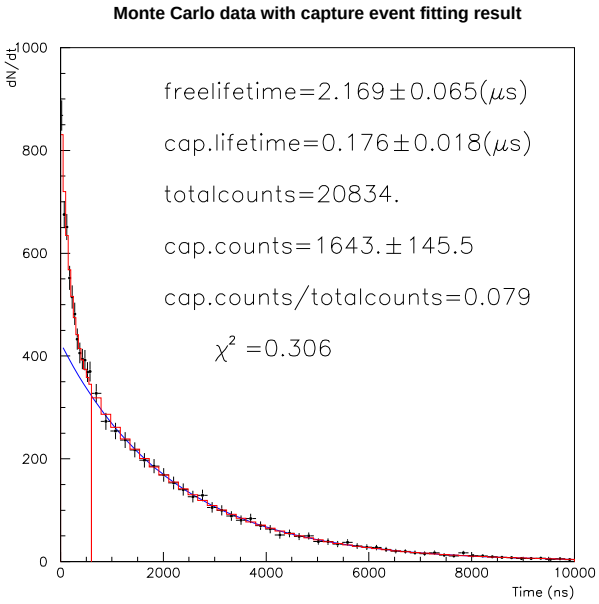

(b) Result of Monte Carlo simulation data with capture event fitting.

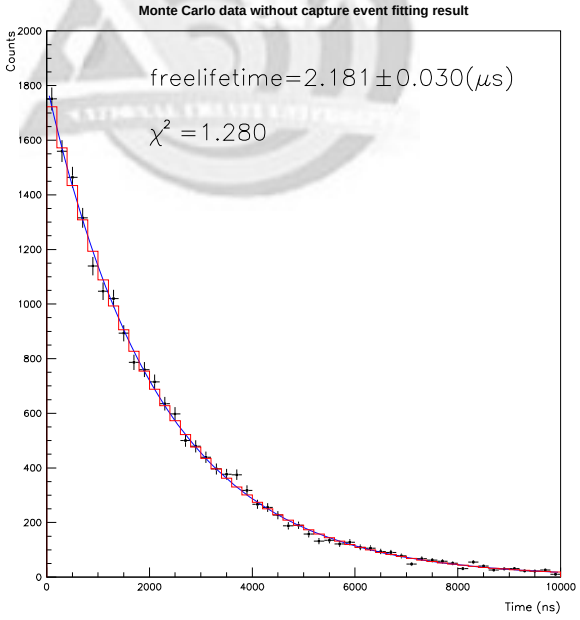

(c) Result of Monte Carlo simulation data without capture event fitting ($y = C_{free}e^{-t/\tau_{free}} + C_{pedestal}$).

Figure 4.4: The fitting result of Monte Carlo data. The results are consistent with the value we set. We think by this check, we can trust our analysis program.

4.3 TDC Data Analysis and Result

In this section the TDC data analysis of this experiment will be presented. We discuss the analysis of changing end point first. Second, we discuss the analysis of changing start point. Finally, the result of TDC data analysis will be presented.

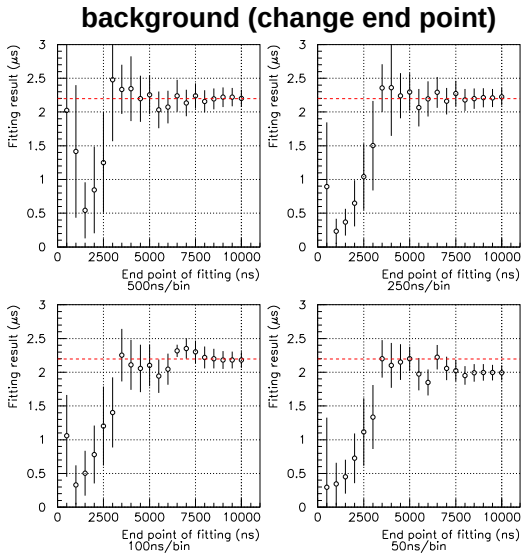

(a) Result of changing the fitting end point without target.

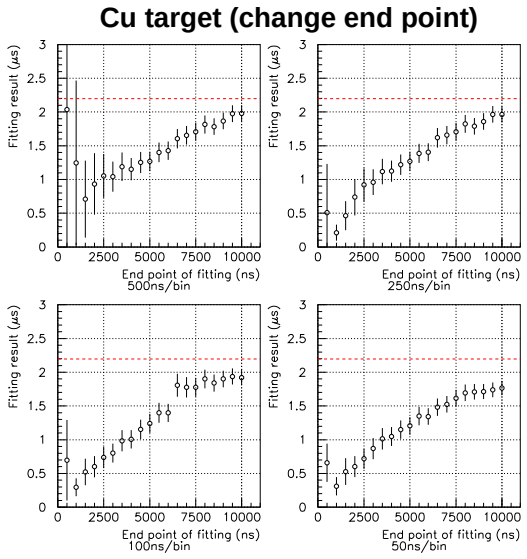

(b) The result of changing the Cu target include data's fitting end point.

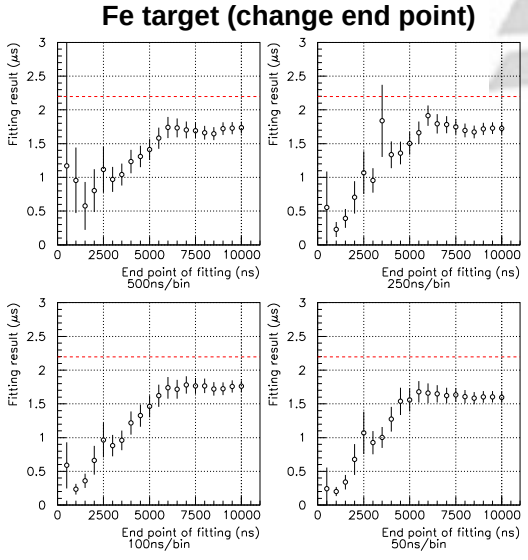

(c) The result of changing the Fe target include data's fitting end point.

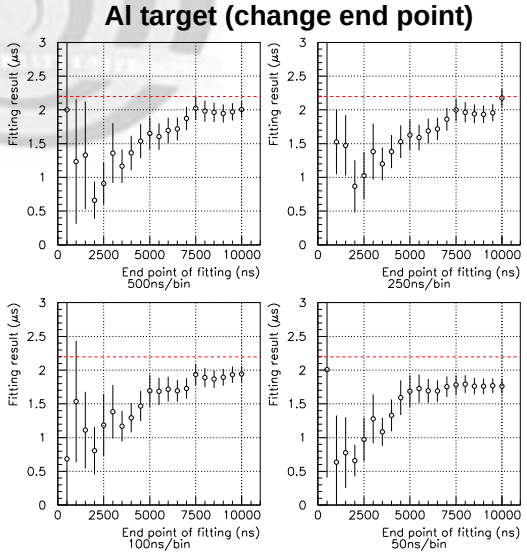

(d) The result of changing the Al target include data's fitting end point.

Figure 4.5: Results of changing the fitting end point of free decay. This fitting is try to find out the suitable end point for free decay part fitting.

FIG. 4.5 shows the results of changing the fitting end point of free decay. The red line in the figure is the world average free decay value. In this step, we also test the influence of different bin size. The subtitle under the figure, like $500ns/bin$ is the bin scale, means the bin size of timing in the TDC distribution.

FIG. 4.5(a) is the result of changing the fitting end point of free decay without target. The

trend become stable in last several points. We can see that the first several points all have huge error bar and the mean value do not have obvious trend to be stable. Because the first several points are the results which having less counts, the error bar will be so huge and the mean value will appear randomly. In order to avoid the effect produced by insufficient statistics, We set the fitting end point in $10000ns$. FIG. 4.5(c) and FIG. 4.5(d) have the same trend in the analysis results. We choose the $10000ns$ to be the end point ,too.

FIG. 4.5(b) is the Cu target including result. We can find that the result shows no gradual trend. We can not clearly understand why there has no gradual trend. Maybe the the stable region will appear after $10000ns$, but our experiment only take the data before $10000ns$. So, We forced the end point to set in $10000ns$.

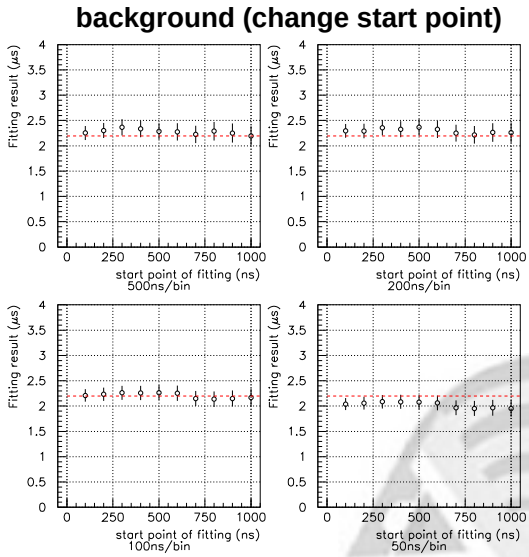

(a) Result of changing the fitting start point without target.

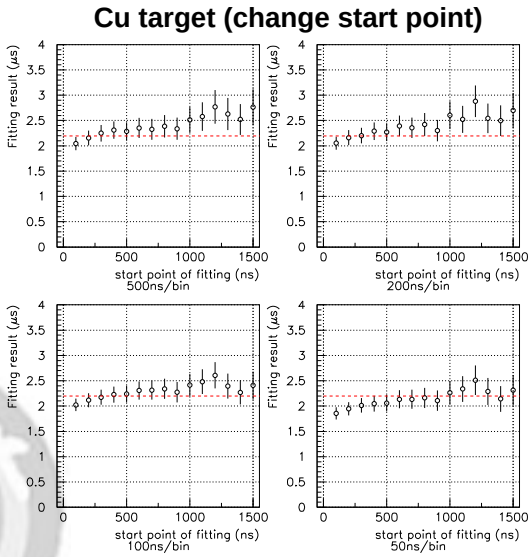

(b) The result of changing the Cu target including data's fitting start point.

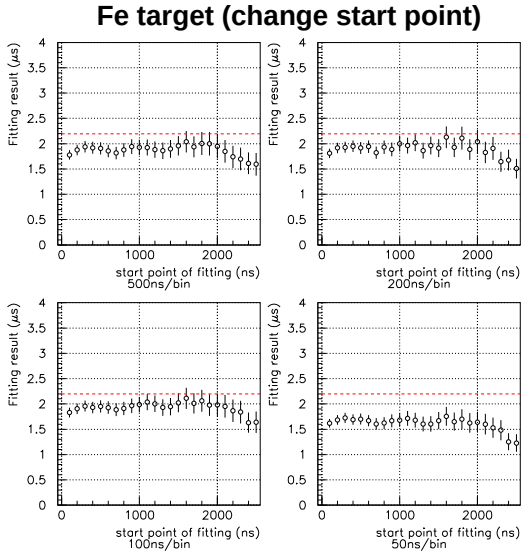

(c) The result of changing the Fe target including data's fitting start point.

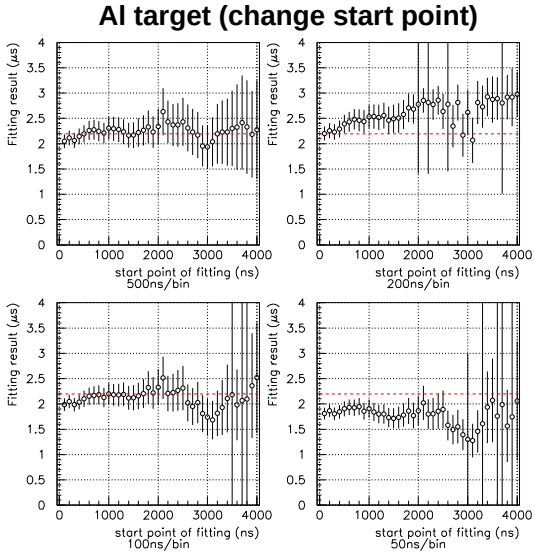

(d) The result of changing the Al target including data's fitting start point.

Figure 4.6: Results of changing the fitting start point of free decay. This fitting is used to find out the suitable start point for free decay part fitting.

From FIG. 4.5(b), FIG. 4.5(c), FIG. 4.5(d) and FIG. 4.5(a) we can find that in the figures labeled "$50ns/bin$" are all have a lower value than other figures. Compare with FIG. 4.2, the figures labeled "$50ns/bin$" are still have a bit lower than others. But this condition is not very obvious in FIG. 4.2. We think it because the FIG. 4.2 are Monte Carlo simulation data which have more than 10 times data than the experiment data. From the comparing with monte Carlo simulation data, We consider it because our data do not have enough amount, if we cut the bins in too small scale, the analysis will lose its preciseness, and reported a low result.

FIG. 4.6 shows the results of changing the fitting start point for free decay. The red line is the muon decay world average value. Like the analysis about finding the end point of free decay part, we also test the influence of different bin size, too.

From FIG. 4.6(a) we can find the result of changing the fitting start point is consistent with the world average. The results in the figure labeled $50ns/bin$ are lower than other figures. The reason of this phenomenon is the same like what we have discussed, but the bin scale is too small.

Let's look at FIG. 4.6(b), FIG. 4.6(c), and FIG. 4.6(d). In this three figures, we choose different time range to analyze the start point of free decay. The reason of this choice is because the study of muon captured lifetime. The world average muon captured lifetime by Cu, Fe, and Al atom are $0.164ns$, $0.201ns$, and $0.880ns$. After calculation, we know that in almost $800ns$, $1000ns$, and $4000ns$ the captured rate by Cu, Fe, Al atom will drop less than 1/100. Because of the different captured lifetime, we choose different range to analyze the data.

FIG. 4.6(c) shows the Fe target inserted result. We can find that all the results are lower than world average. We think this phenomenon come from the impurity in the target. From the supplier, the Fe target's purity is only about 90%. The Cu and Al target's purity are about 99.7%.

FIG. 4.6(b) and FIG. 4.6(d) are the results of changing the fitting start point with Cu and Al target. We can see that the first several point of the results are all lower than the world average. The reason of this phenomenon is because the data contain the captured events. Comparing with FIG. 4.5(b), FIG. 4.5(c), and FIG. 4.5(d), all the results are lower than the world average have the same reason.

We choose $600ns$ to be the start point of free decay for the without target including data. $800ns$, $1000ns$, $2000ns$ for Cu, Fe, Al target including data. Although, from the study, the captured events of Al atom will lower than 1% after $4000ns$. But, from FIG. 4.6(d) we can find the trend after $2000ns$ become unclear. We think, the phenomenon is come from the insufficient statistics. So, we choose $2000ns$ to be the start point of free decay part.

FIG. 4.6 are the results of fitting. All the fitting result are listed in Table .4.1.

Table 4.1: The results of TDC data analysis.

Target	free decay lifetime	capture decay lifetime	capture decay world average	capture counts
Cu	$2.308 \pm 0.298\mu s$	$0.351 \pm 0.084\mu s$	$0.164 \pm 0.002\mu s$	192
Fe	$2.111 \pm 0.346\mu s$	$0.258 \pm 0.094\mu s$	$0.201 \pm 0.004\mu s$	181
Al	$2.251 \pm 0.714\mu s$	$0.756 \pm 0.215\mu s$	$0.880 \pm 0.011\mu s$	255
background	$2.226 \pm 0.130\mu s$			

From the result we can see that the fitting result of captured lifetime have a large error bar. In order to decrease the error bar we cut the bins in small time scale. But it still very large

relative to the mean value. We think it because the data amount is too less. If we want to increase the quality of this fitting, we must get more data.

FIG. 4.7(a) is the result of fitting without any target including. It should have no captured lifetime. But we can find that there is a $0.198ns$ captured lifetime component were be fitted. Look back on the FIG. 3.3, it's the structure of detector. If we do not insert the target metal between layer 2 and layer 3, there will only have the air. In our opinion the captured event may come from the atom of air and layer 2 scintillator. But we believe that this effect can be neglected in other measurement. Because the other data with target including are acquired for 5 days, but the data without target are acquired for almost 13 days. The rate of captured by air and scintillator atom is lower than the target captured rate.

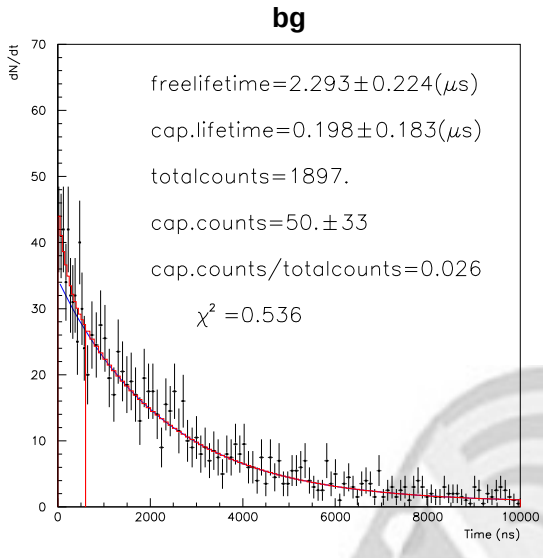

(a) Result of fitting without target.

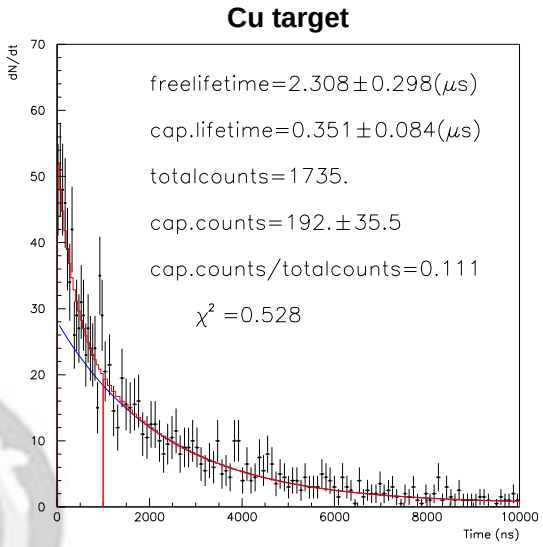

(b) The result of Cu target including data.

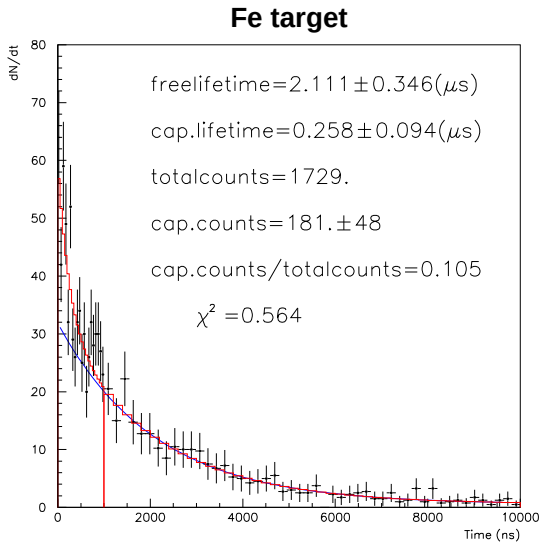

(c) The result of Fe target including data.

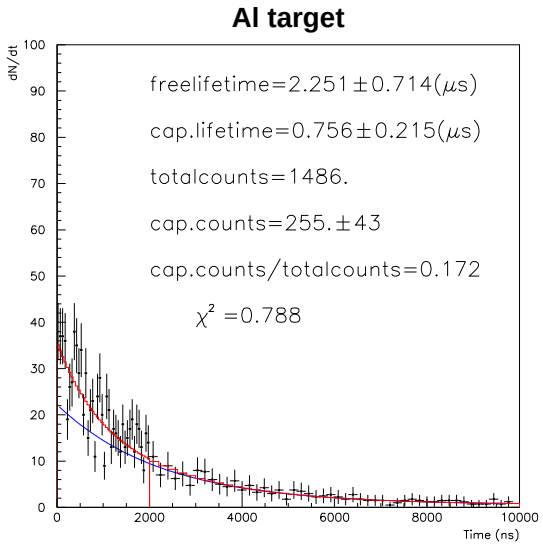

(d) The result of Al target including data.

Figure 4.7: Results of fitting. The capture lifetime fitting result of Cu, Fe, and Al target include data are $0.351 \pm 0.084\mu s$, $0.258 \pm 0.094\mu s$, and $0.756 \pm 0.215\mu s$.

Another conjecture about the captured lifetime component is the fitting function. In this re-

sult of fitting without any target including we use the function $y = C_{free}e^{-t/\tau_{free}} + C_{cap.}e^{-t/\tau_{cap.}} + C_{pedestal}$. The analysis program may forced to fit the data in a the form which with captured lifetime component. We try to fit the data using the function $y = C_{free}e^{-t/\tau_{free}} + C_{pedestal}$. The muon free decay lifetime is presented in FIG. 4.8. We can see that the muon free decay lifetime is $2.226 \pm 0.130\mu s$. Whin error bar, comparison with the result in FIG. 4.7(a) is consistent.

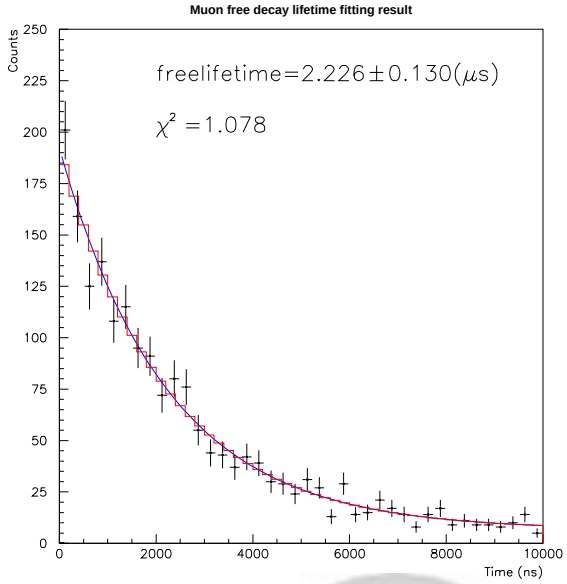

Figure 4.8: The muon free decay lifetime fitting result. This result is fitted by the function $y = C_{free}e^{-t/\tau_{free}} + C_{pedestal}$ which with no capture component.

The Cu target fitting result is presented in FIG. 4.7(b). The muon captured lifetime is $0.351 \pm 0.084\mu s$. Comparing with the world average value 0.164 ± 0.002, we can see that within error bar our fitting result is still large than world average. We think the error may come from our experiment systematic error. Just now we can not explain this phenomenon.

FIG. 4.7(c) shows the fitting result of the Fe target include data. Within error bar, the captured lifetime $0.258 \pm 0.094\mu s$ is close to the world average $0.201 \pm 0.004\mu s$.

FIG. 4.7(d) shows the fitting result of the Al target include data. Within error bar the result are consistent with the world average. But, comparing the capture event counts with FIG. 4.7(b) and FIG. 4.7(c). The trend of capture event counts is not consistent with the theory prediction[8]. The capture event counts for Cu, Fe, and Al target is 192 ± 35,181 ± 48, and 255 ± 43. From the theory, the probability for muon captured by nuclei is proportional to Z^4, Z is the atomic number of nuclear. The Cu and Fe's atomic number is bigger than Al's. According to the theory, the capture event counts of Al target must be the less one. But our fitting results shows the different trend. We still can not explain this phenomenon now. Maybe we should take more Al target data to increase the precision of fitting.

4.4 ADC Data Analysis and Results

We are try to use the ADC data to distinguish the capture decay event and free decay event. The ADC data analysis of this experiment are presented in this section.

FIG. 4.9 and FIG. 4.10 are the profile figure of ADC VS. TDC. Fig. 4.9 is without TDC cut. Because the capture decay events of the select target in this experiment are more visible in TDC$<1000ns$. We draw a figure which have a TDC cut in $1000ns$, FIG. 4.10 is the result. Unfortunately, the profile figures do not have clear evidence about the two kinds of decay events. We can not recognize the capture decay event and free decay event by this method. We are going to try other methods.

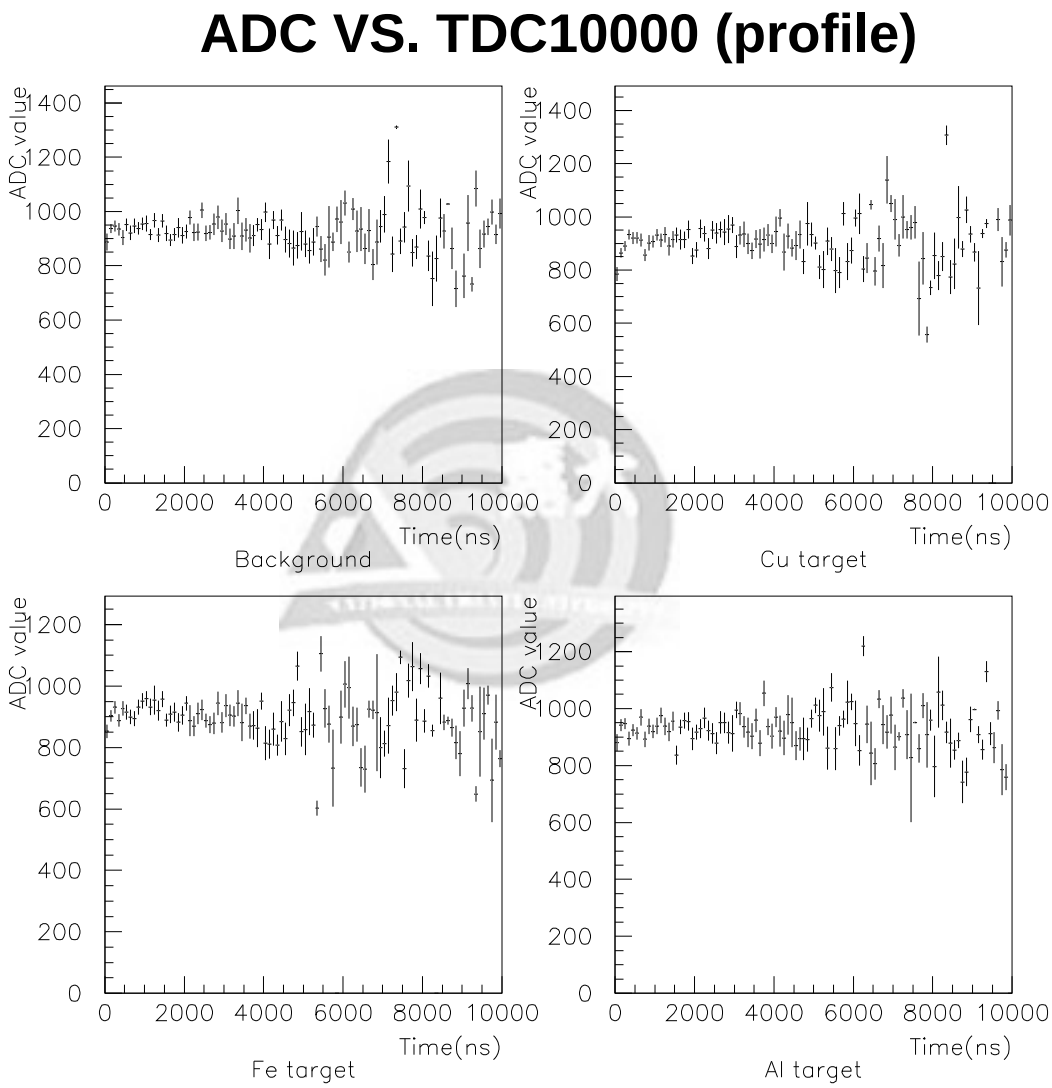

Figure 4.9: ADC VS. TDC profile analysis result. This analysis shows all the TDC without any cut.

FIG. 4.11 shows the results of probability of compatibility between two ADC histograms using the Kolmogorov test[12]. This test is a statistical test of compatibility in shape between two histograms. FIG. 4.11(a) shows the TDC$<1000ns$ data. FIG. 4.11(b) shows the comparison of FIG. 4.11(a) which TDC$>1000ns$. In the left up of this two figure is the measurement without target including, we call this data background, and others are Cu, Fe, and Al target data. The "Prob." is the probability of compatibility between two histograms, one is the data

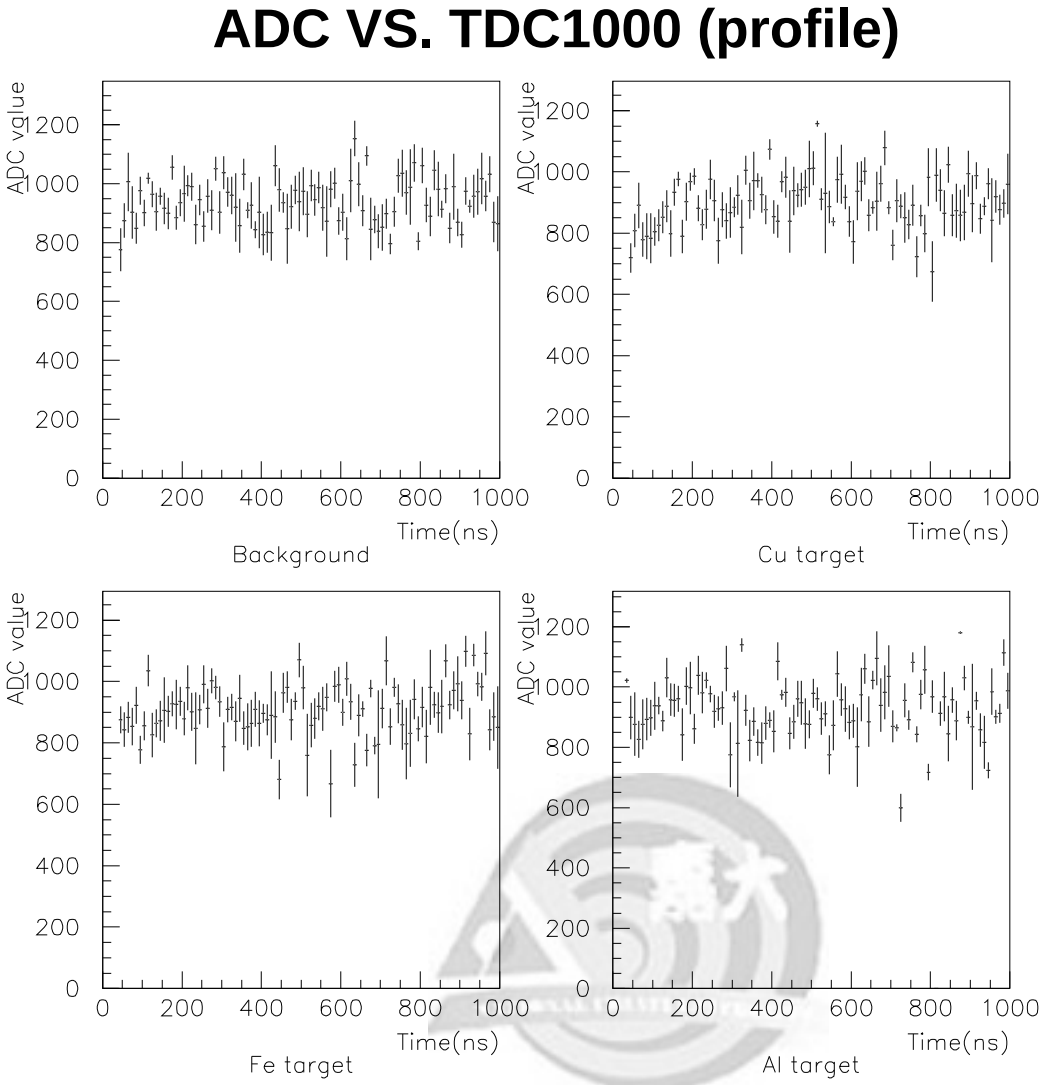

Figure 4.10: ADC VS. TDC profile analysis result (TDC< 1000). In order to find out the captured events we focus on the range where TDC< 1000ns

without target include and the other is the Cu, Fe, and Al target data. The probability is defined between 0 to 1, the result equal to 1 means the histogram have highly probability that they could come from the same parent distribution.

Table .4.2 lists the results. we can see that the Al target events are highly similar in different TDC cut. But others are not. We conjecture that the Al data can so similar is because the capture probability of Al atom is less than the other two atom.

The capture probability is depend on the the atomic number. The more atomic number, the highly capture probability. Al target event may have too less capture events because its difference with the histogram without target including is not clearly. But, the Cu and Fe target events are not. Back to the Table .4.2, unfortunately, although the Cu and Fe events have strong difference with background, but there have no consistency between them. We can see that in the analysis of TDC< 1000ns, the probability of compatibility between Cu data and background data is only 0.01, but between Fe data and background is 0.045. And, in TDC> 10000ns, the probability of compatibility between Cu data and background data is 0.064. The probability between Fe data and background is 0.006. We only can say that the Cu and Fe target include data may have strong difference with background data, but we can not

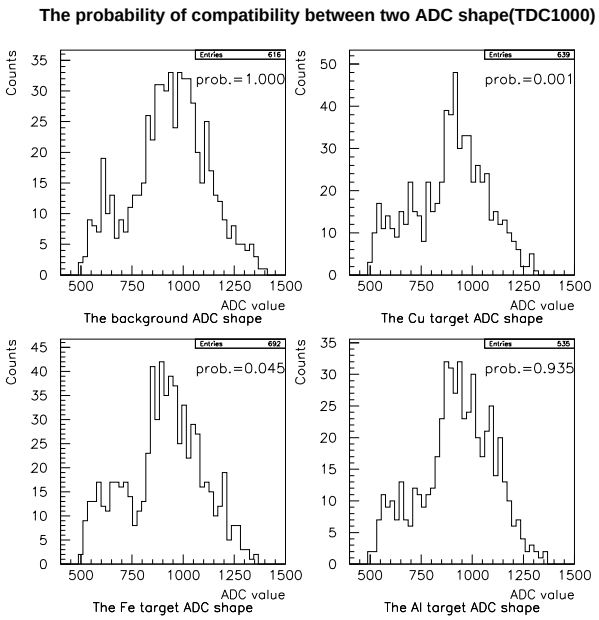

(a) Probability of compatibility between two ADC histogram(TDC< 1000).

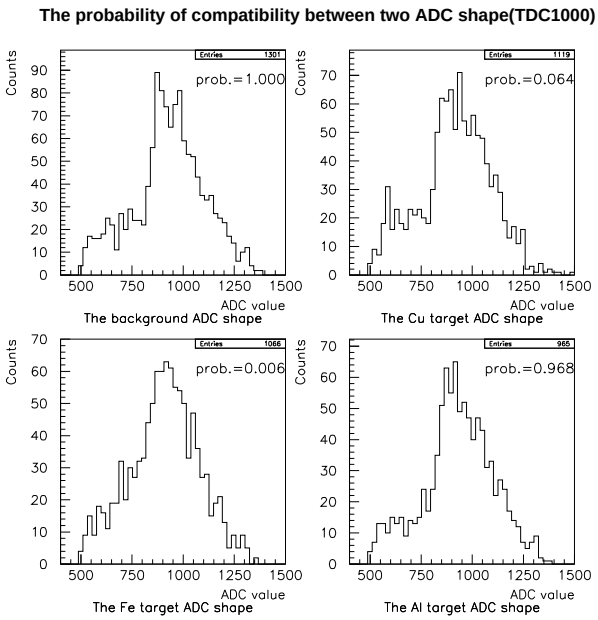

(b) Probability of compatibility between two ADC histogram(TDC> 1000).

Figure 4.11: The result of probability of compatibility test. In this test, we try to compare the probability of compatibility in different TDC range to find if there is any evidence can separate the captured events and free decay events.

Table 4.2: The results of probability of compatibility between two ADC histogram.

Target	Prob.(TDC< $1000ns$)	Prob.(TDC> $1000ns$)
background	1	1
Cu	0.01	0.064
Fe	0.045	0.006
Al	0.935	0.968

recognize them. We think analysis still can not separate the two kinds of decay events. We need to try another method.

The last method we try to separate the two kinds of decay events is to divide the data by different ADC cut and fit the TDC data to get the timing information. After we cut the data by different ADC cut, we use the method introducing in section .4.3 to fit the TDC data and try to find if there have any evidence can separate the two kinds of events.

FIG. 4.13 - FIG. 4.16 are the TDC data fitting results of cut the data by different ADC cut. We choose three different ADC cuts in this analysis 800, 910 950, and 1060. FIG. 4.12 is the ADC distribution histogram. The three different color lines red, green, and blue cut in different ADC value. The red line cuts in 800. We can see the ADC distribution in the front of ADC value 800 and in the back of ADC value 800 have a strong difference. The green line means the cut between 910 to 950, it will cut in different ADC value in different target. In background, the green line cut in 940. In Al target, the green line cut in 950. In Cu and Fe target, the green line all cut in 910. The reason of choose the different cut is to balance the event counts. The blue line cuts in the ADC value 1060. In the figure, we can see the ADC

distribution also difference in the front of 1060 and in the back of the ADC value.

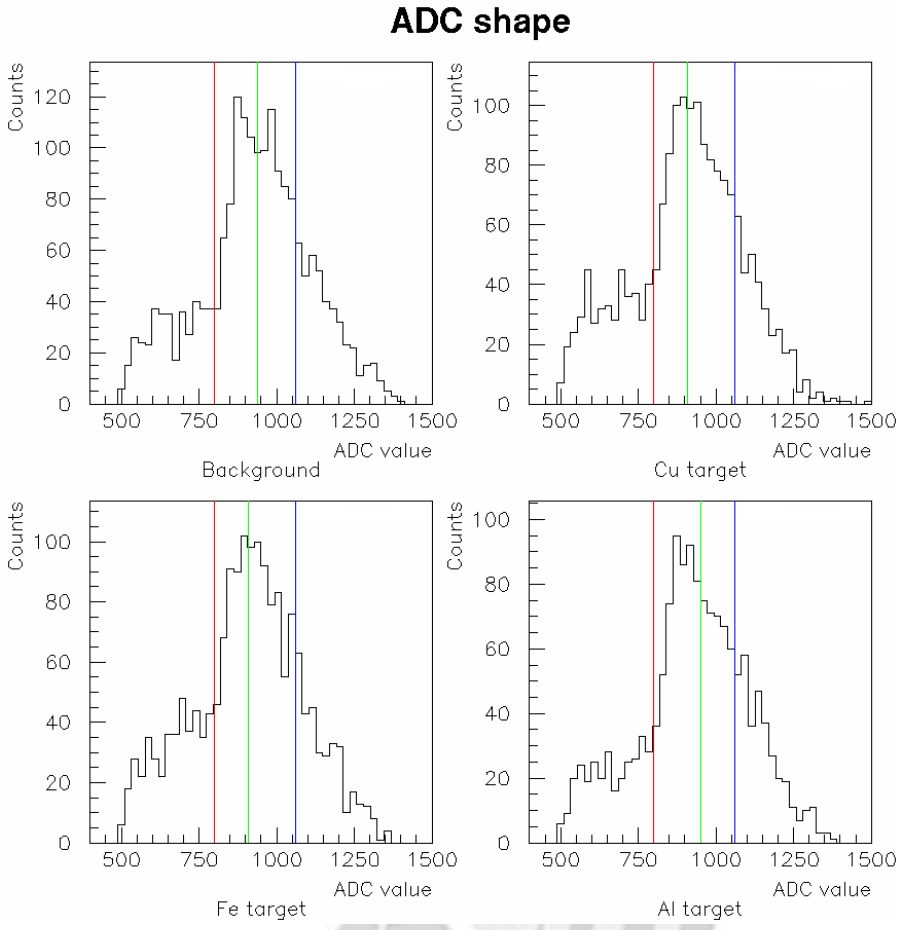

Figure 4.12: The ADC shape. In this figure the three different color line label the ADC cut point.

FIG. 4.13 shows the result of the data without target. We can see that all the captured lifetime have a huge error bar relative to the mean value. Because there have no target, and the captured lifetime produced by the air and scintillator atom are rare, the error bar will become very large.

FIG. 4.14 are the results of the data with Cu target. First, let us focus on the FIG. 4.14(a) and FIG. 4.14(f), we can see the fitting result of free decay lifetime in this two analysis are fail. The reason of this phenomenon is because the insufficient statistics which we have discussed in section. 4.3. The insufficient statistics will decrease the value of fitting result. The FIG. 4.15(f) and FIG. 4.16(a) have the same phenomenon. Because the fitting is fail, We do not discuss about this kinds of data and its corresponding data.

From FIG. 4.14(c) and FIG. 4.14(d), we can find within error bar, both of these two fitting result can be close to the world average. The captured event counts are similar to each other and the ratio of captured events to total counts are similar, too. We think the muon captured events are uniform spread in every ADC cut.

FIG. 4.15 are the results of the data with Fe target. We can find the captured lifetime error bar in FIG. 4.15(b) is too huge. The huge error bar means the captured lifetime may be any value between the error bar. And the huge error bar of captured lifetime will influence the capture event counts. We can find the capture event counts have a huge error bar, too. The reason of the so big error bar may come from the insufficient statistics and systematic error. The too less counts cause the mean value in the first several bins are disorder. The disorder

of the first several bins will lead the fitting fail. We believe that this kinds data should not be consider.

Compare the two figure FIG. 4.15(c) and FIG. 4.15(d). The captured lifetime within error bar can satisfy grudgingly. The big captured lifetime error bar in FIG. 4.15(d) may come from the same reason which we have discussed in last paragraph, insufficient statistics and systematic error. The ratio of captured event counts to total event counts are close. Like the discussion result of FIG. 4.14(c) and FIG. 4.14(d), we think the muon captured events are uniform spread in every ADC cut.

FIG. 4.16 are the results of the data with Al target. Consider the figures FIG. 4.16(c) and FIG. 4.16(d), like the FIG. 4.15(c) and FIG. 4.15(d), the captured lifetime within error bar can satisfy grudgingly. And the ratio of captured event counts to total event counts are very close. Like we have discussed, we think the muon captured events are uniform spread in every ADC cut. In FIG. 4.16 we can see that the first several bins' scale are bigger than Cu and Fe target include data. Because the over all counts of Al target include data is less than Cu and Fe data. If we tune the scale like the Cu and Fe target include data, the fitting will fail swiftly. So, we must use a bigger scale in the first several bins. The big bin scale may cause the error bar to be large. We think this is a reason about the big error bar in this two capture lifetime fitting results.

Within error bar the captured lifetime fitting results of FIG. 4.16(e) and FIG. 4.16(f) can be close. But the ratio of captured event counts to total event counts is different obviously. The result in FIG. 4.16(e) is 0.057 and in FIG. 4.16(f) is 0.178. From the result we can find in FIG. 4.16(f) the ratio of captured event counts to total event counts is higher than FIG. 4.16(e). By this analysis result, the capture events may have more chance to occur in the region of high ADC value. But consider with the capture event counts error bar. The error bar is too big, within error bar we even can change the result. We think this phenomenon can be a hint to find the correspond between the captured event counts and ADC value. But in this experiment, the counts is too less, we can not confirm its a real physic phenomenon or an error by insufficient statistics and systematic error.

From the discussion in Cu, Fe, Al target including data, we can get a conclusion that the probability of muon captured data may uniform spread in every ADC cut is higher than the captured events occur in high ADC value region.

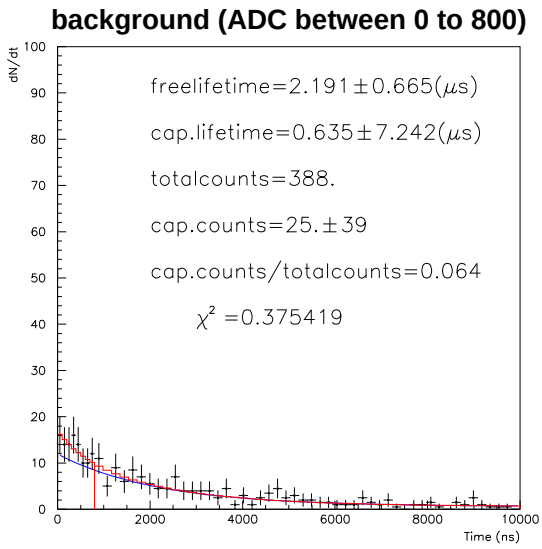

(a) ADC cut between 0 to 800.

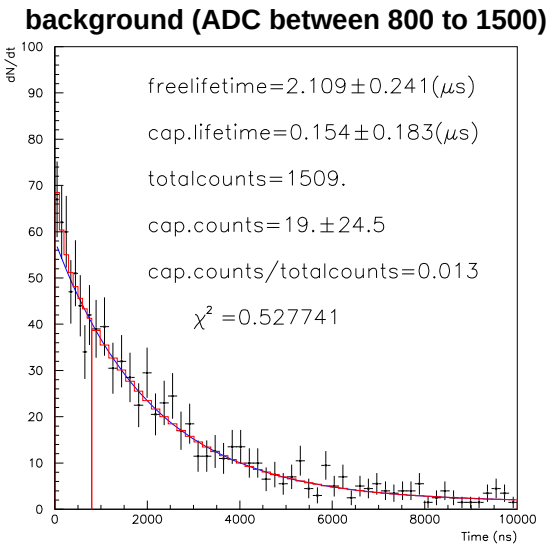

(b) ADC cut between 800 to 1500.

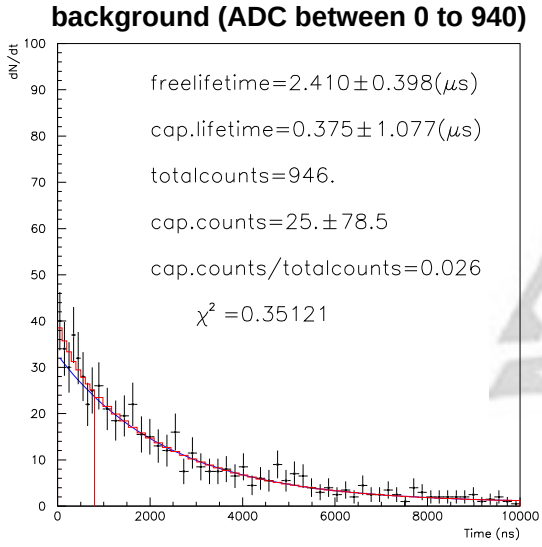

(c) ADC cut between 0 to 940.

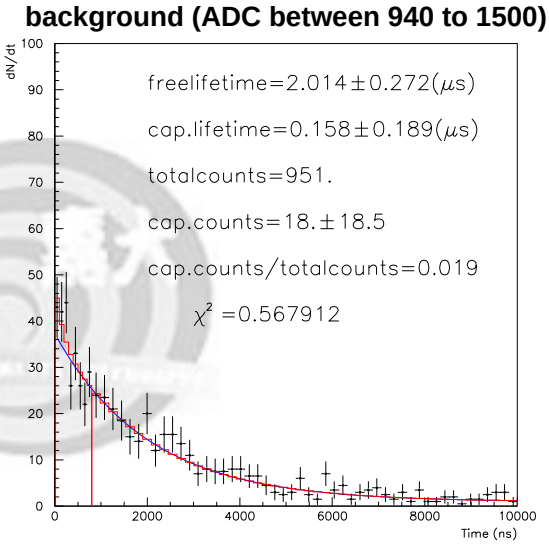

(d) ADC cut between 940 to 1500.

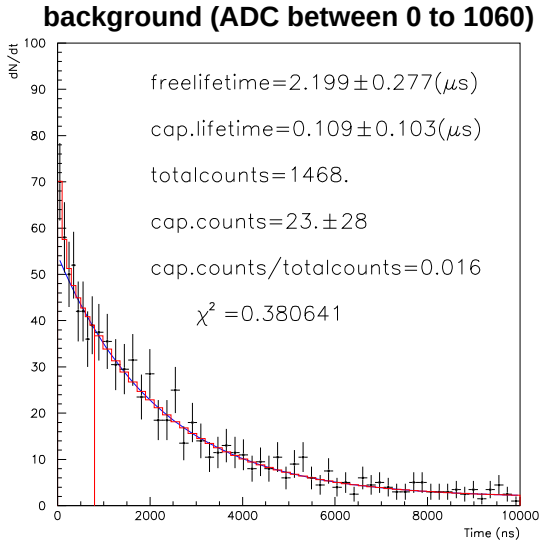

(e) ADC cut between 0 to 1060.

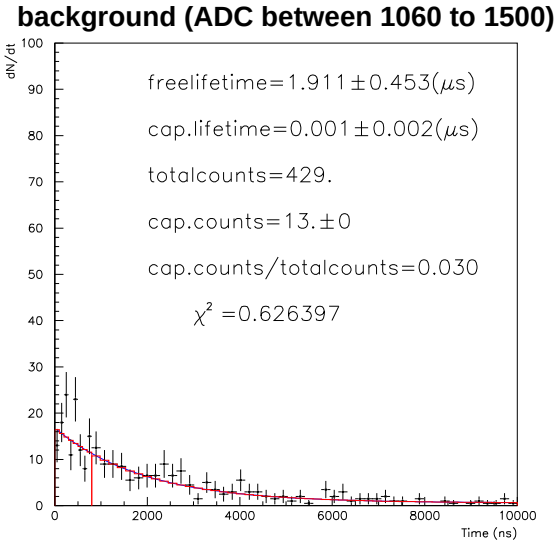

(f) ADC cut between 1060 to 1500.

Figure 4.13: Different ADC Cut for the data without target.

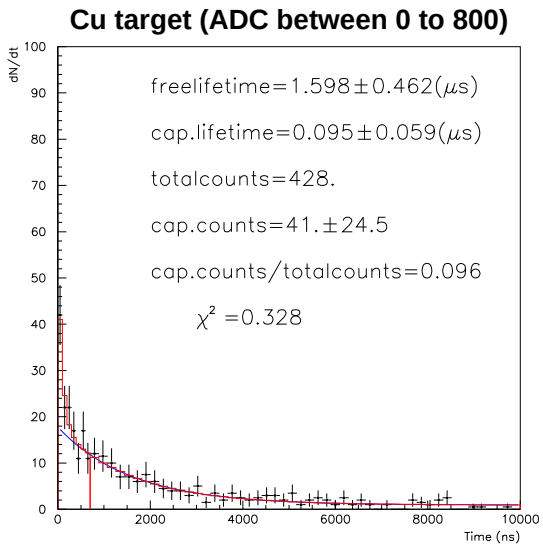

(a) ADC cut between 0 to 800.

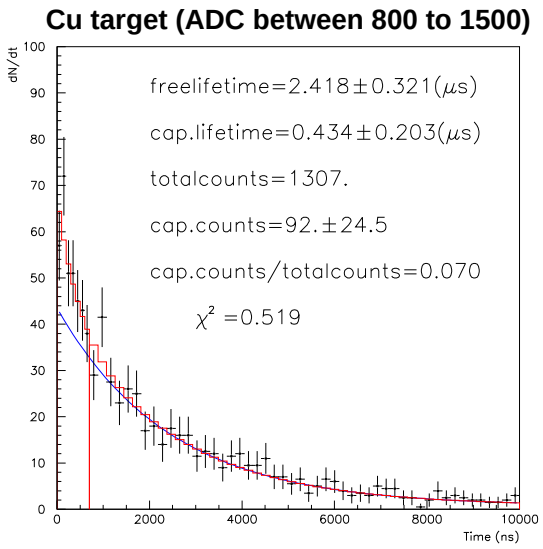

(b) ADC cut between 800 to 1500.

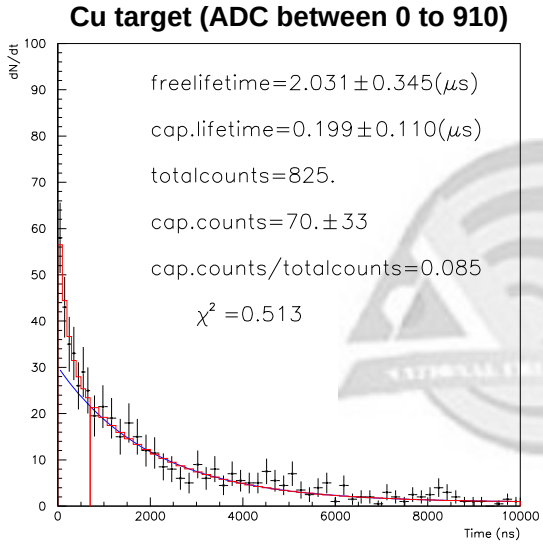

(c) ADC cut between 0 to 910.

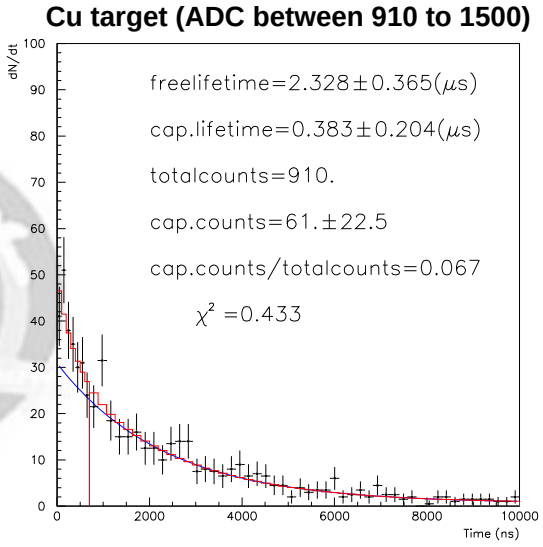

(d) ADC cut between 910 to 1500.

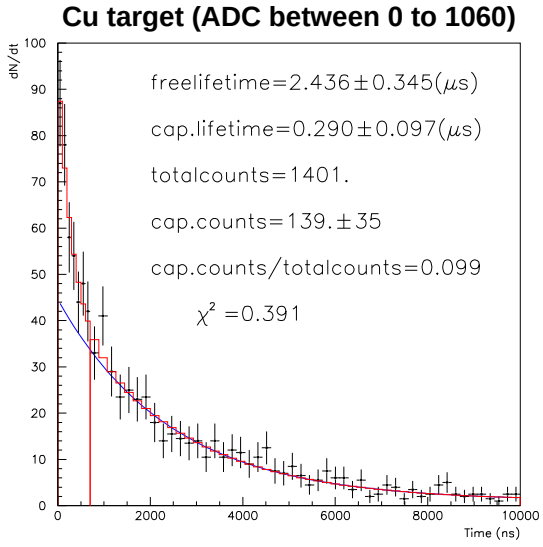

(e) ADC cut between 0 to 1060.

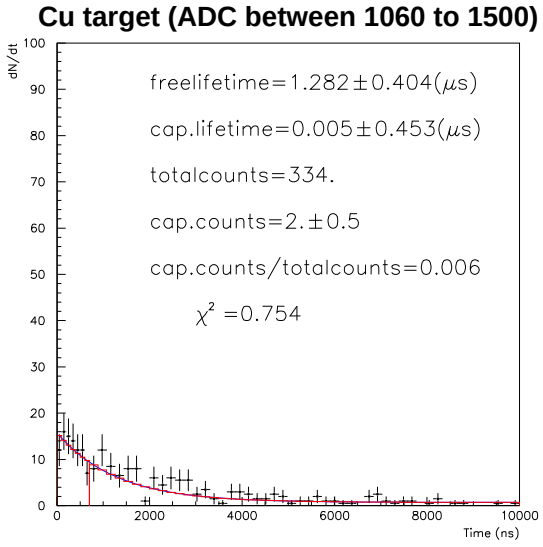

(f) ADC cut between 1060 to 1500.

Figure 4.14: Different ADC Cut for the data with Cu target.

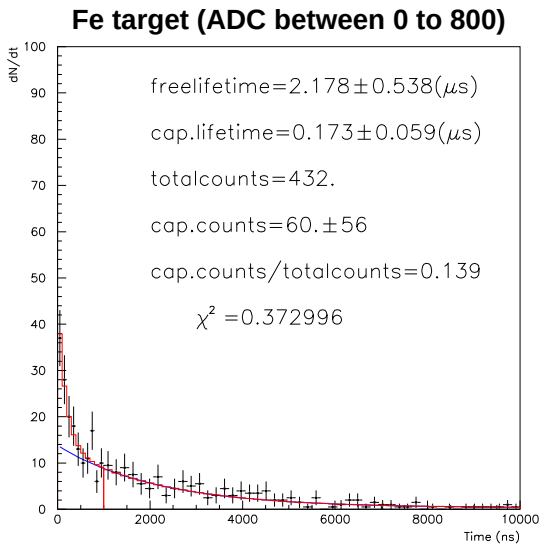

(a) ADC cut between 0 to 800.

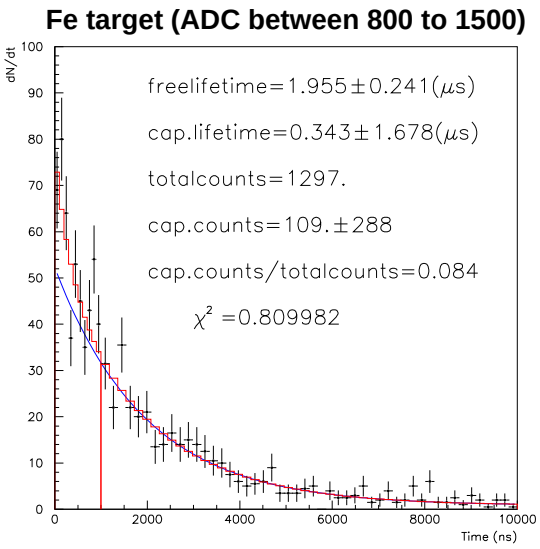

(b) ADC cut between 800 to 1500.

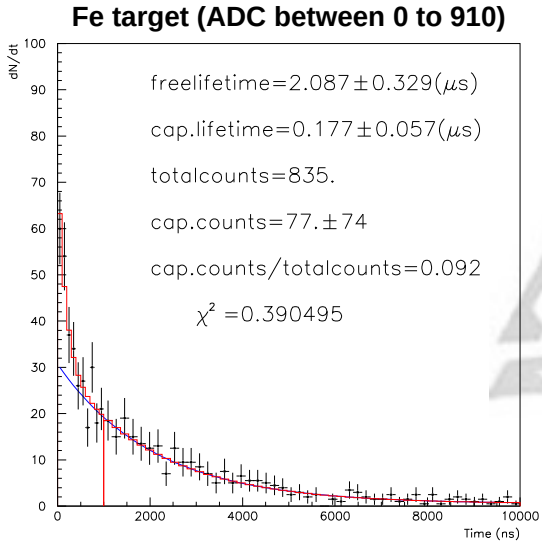

(c) ADC cut between 0 to 910.

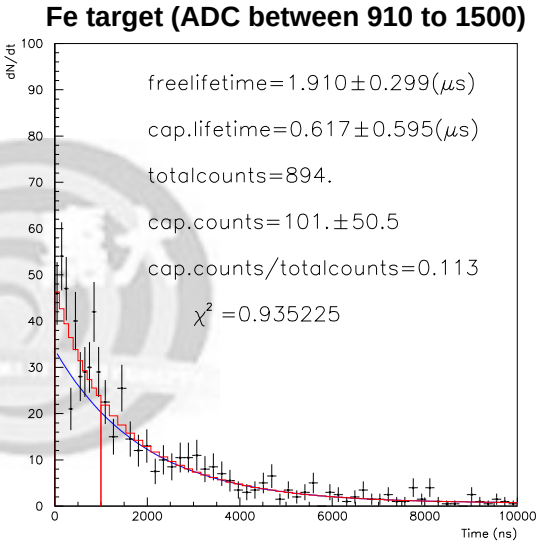

(d) ADC cut between 910 to 1500.

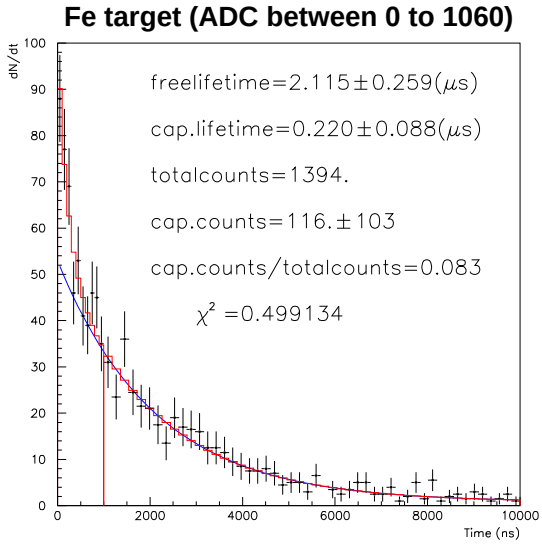

(e) ADC cut between 0 to 1060.

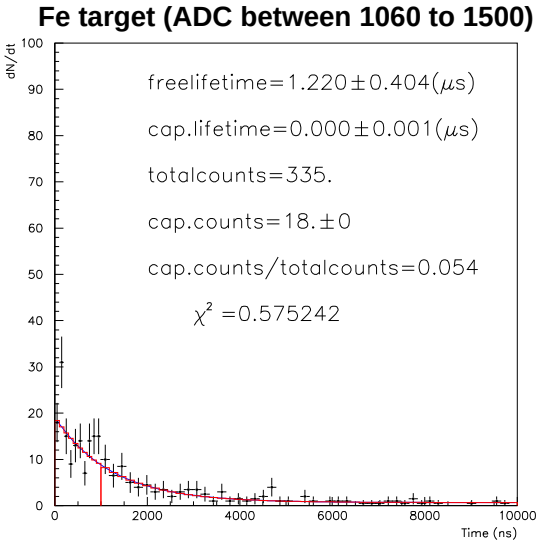

(f) ADC cut between 1060 to 1500.

Figure 4.15: Different ADC Cut for the data with Fe target.

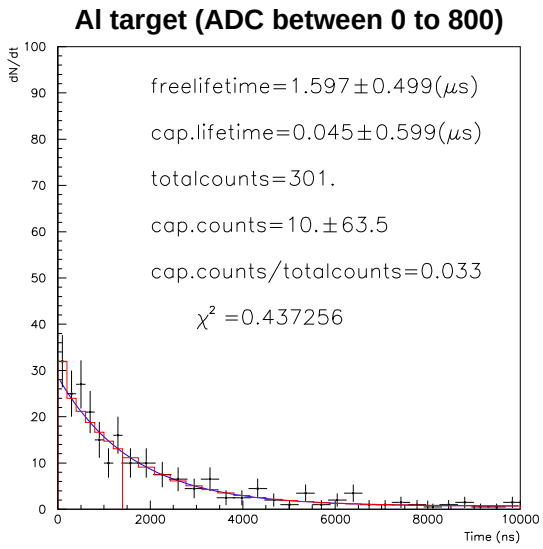

(a) ADC cut between 0 to 800.

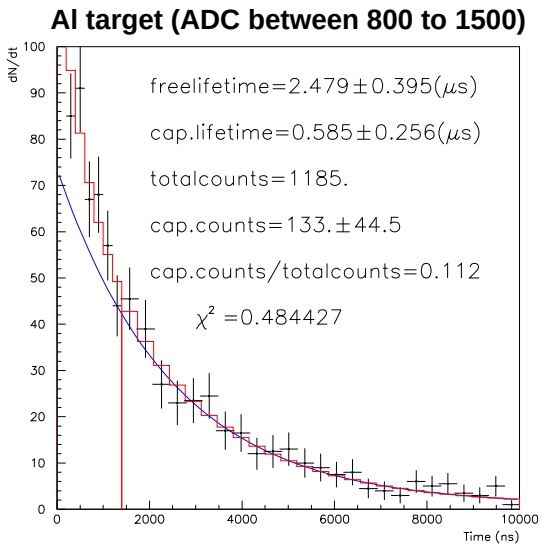

(b) ADC cut between 800 to 1500.

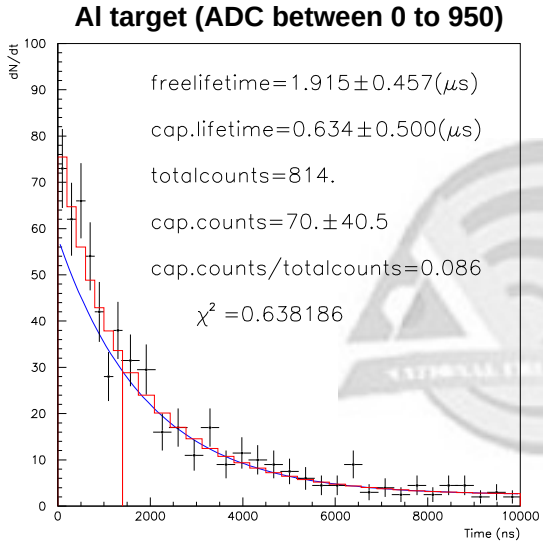

(c) ADC cut between 0 to 950.

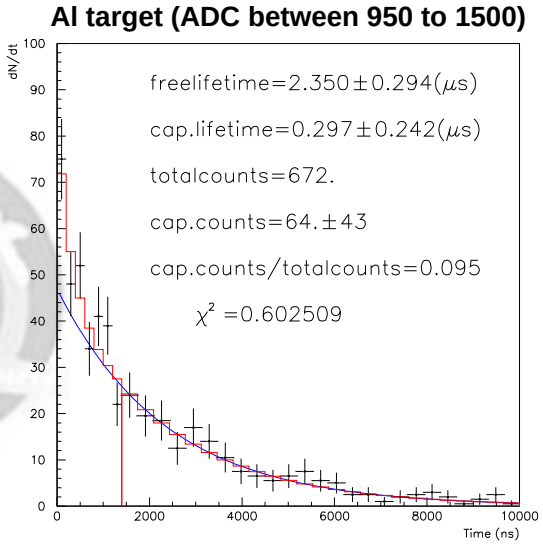

(d) ADC cut between 950 to 1500.

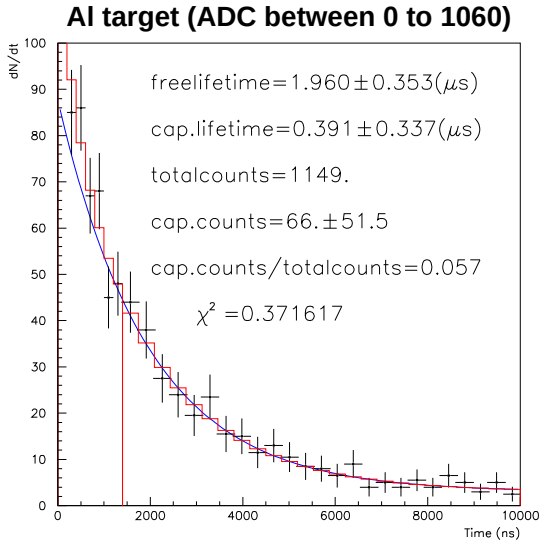

(e) ADC cut between 0 to 1060.

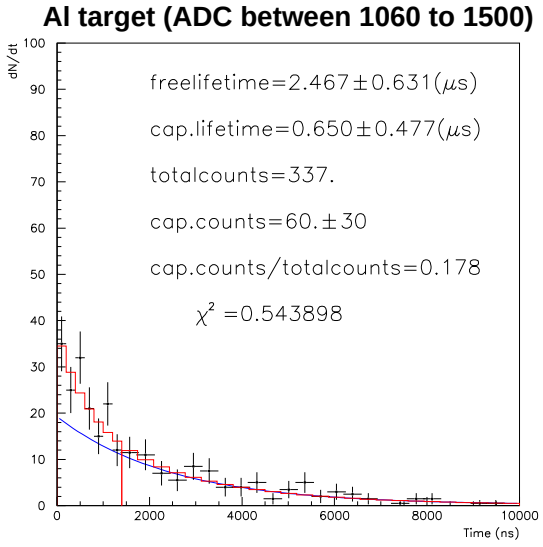

(f) ADC cut between 1060 to 1500.

Figure 4.16: Different ADC Cut for the data with Al target.

Chapter 5

Conclusion

In this experiment, we use the cosmic ray to be the source, and plastic scintillator to be the detector, and adding a target metal, to measure the muon capture phenomenon. But the capture rate is low. The detection rate is approximate to 4.41×10^{-4} per cm^2 per min.

The captured muon lifetime for Cu, Fe, and Al was experimentally determined to be $0.351 \pm 0.084\mu s$, $0.258 \pm 0.094\mu s$, and $0.756 \pm 0.215\mu s$. The world average value are $0.164 \pm 0.002\mu s$, $0.201 \pm 0.004\mu s$, $0.880 \pm 0.011\mu s$. The muon free decay lifetime is $2.226 \pm 0.130\mu s$. The world average is $2.197 \pm 0.00037\mu s$.

The differences in the values may come from impurity in the target, insufficient statistics, and systematic error.

From some reference, it notes that the output pulse shape of plastic scintillator by detecting the electron and the proton is not the same. But in this experiment, we prove that using the traditional Analog to Digital Converter(ADC) to measure the pulse's charge information can not differentiate it.

To improve the results we recommend using high-flux muon source to replace the cosmic ray source, and using a Flash Analog to Digital Converter(FADC) to measure the full pulse information to replace the traditional ADC.

This experiment is a good training for students who want to contact the high energy physics first. In this experiment students can learn how to design a high energy physics experiment, the experiment methods and the fitting technology. It's useful for students to do the further research in any field of physics.

Appendix A

Visual Basic Program

This program can download from:
http://www.phys.sinica.edu.tw/∼spring8/users/shshiu/program/vbprogram.zip The following is the program code.

```
Dim buffer1 Dim buffer2 Dim tired Dim even Dim recy Dim pres Dim
chan1 Dim chan2 Dim modein Dim mode1 Dim aaut



Private Sub cleartex2_Click() Text2 = ""

buffer1 = "" End Sub

Private Sub cletex1_Click() Text1 = "" End Sub

Private Sub Chiu_Click() Dim chiu 'As String aaut = "auto?" chiu =
"clea;mode 0,0;mode 1,13;evts;pres 1;recy 0.01;even 99999999;chan
1,-0.100;chan 2,-0.100;*lrn?" chiu = chiu + vbCr + aaut + vbCr
MSComm1.Output = chiu End Sub



Private Sub mode_Click() Dim modetest 'As String

modetest = "mode?" modetest = modetest + vbCr MSComm1.Output =
modetest 'Text3.Text = MSComm1.Input

End Sub


Private Sub Option1_Click() modein = 9 End Sub

Private Sub Option2_Click() modein = 10 End Sub

Private Sub Option3_Click() modein = 11 End Sub

Private Sub Option4_Click() modein = 12 End Sub
```

```
Private Sub Option5_Click() modein = 13 End Sub

Private Sub Send_Click() Dim tmp 'As String buffer2 = buffer2 + tmp

    tmp = (Text1.Text)
    tmp = tmp + vbCr

    MSComm1.Output = tmp

'MSComm1.Output = Text1.Text End Sub



Private Sub idn_Click() Dim idntest 'As String idntest = "*idn?"
idntest = idntest + vbCr MSComm1.Output = idntest End Sub

Private Sub Form_Load() tired = 0

Text1.Text = "Try to enter something here" Text2.Text = "Response"
If MSComm1.PortOpen = False Then MSComm1.PortOpen = True
Timer1.Interval = 50 MSComm1.Output = Chr(17) End Sub

Private Sub single_Click() Dim sin 'As String aaut = "auto?" even =
"even" & " " & (eventex.Text) recy = "recy" & " " & (recytex.Text)
pres = "pres" & " " & (prestex.Text) chan1 = "chan 1," &
(chan1tex.Text) chan2 = "chan 2," & (chan2tex.Text) mode1 = modein
sin = "clea;mode 0,0;evts;mode 1," & mode1 & ";" & chan2 & ";" &
chan1 & ";" & pres & ";" & recy & ";" & even & ";" & "*lrn?" sin =
sin + vbCr + aaut + vbCr MSComm1.Output = sin End Sub

Private Sub START_Click() MSComm1.Output = Chr(20) End Sub

Private Sub STOP_Click() MSComm1.Output = Chr(18) End Sub

Private Sub Delay(ASecond As Integer)
    Dim before
    before = Timer
    Do
    DoEvents
    Loop Until (Int(Timer - before) = ASecond)
End Sub

Private Sub stopcount_Click() Dim stc 'As String stc = "stop" stc =
stc + vbCr MSComm1.Output = stc End Sub

Private Sub Text2_Change() Text2.SelStart = Len(Text2.Text) End Sub


Private Sub Timer1_Timer() Dim str 'As String Dim majorbuffer
FCOM1.Caption = "NOW THE TIME IS" & Date & Time majorbuffer =
```

```
MSComm1.Input Dim fs, f

 Const ForReading = 1, ForWriting = 2, ForAppending = 8
 Const TristateUseDefault = -2, TristateTrue = -1, TristateFalse = 0
 Dim FN As String
  FN = ".\FILE\" & _
       Year(Date) & "_" & _
       Month(Date) & "_" & _
       Day(Date) & "_" & _
       Hour(Time) & "_" & _
       ".txt"

buffer1 = buffer1 + majorbuffer str = str + buffer1 If Len(str) > 0
Then Text2.Text = str Set fs =
CreateObject("Scripting.FileSystemObject")

      If fs.FileExists(FN) = False Then
         Set f = fs.CreateTextFile(FN, True)
         f.Close
         End If

      Set f = fs.OpenTextFile(FN, ForAppending, TristateFalse)
      f.Write (majorbuffer)
      f.Close
End Sub


Private Sub Xoff_Click() MSComm1.Output = Chr(19) End Sub

Private Sub Xon_Click() MSComm1.Output = Chr(17) End Sub
```

Appendix B

Monte Carlo Simulation Program

This program can download from:
http://www.phys.sinica.edu.tw/∼spring8/users/shshiu/program/muon.c The following is the program code.

```
#include<stdio.h>
#include<stdlib.h>
#include<math.h> FILE
*filewrite;

int main(void) {
  int data[22000], intermed;
  int index;
  srand((int) time(0));
  filewrite = fopen("vmesavefile1","a+");

  for(index=1;  index<=20000; index++)
    {
      /* intermed = rand()/3276.7;
     data[index]=-2197.00*log((double)(intermed/2197.00));
     printf("%lf \n",data[index]);
     printf("%lf \n",data[index]);*/

      intermed=rand()%(20000-211+1)+211;
      /*data[index]=-2197*log((intermed)/4000);*/
      data[index]=-2197.00*log(intermed/20000.00);
      /* jeng=abs(data[index]);*/
      printf("time=%d \n",index);
      printf("rand=%d \n",intermed);
      printf("exp=%d \n",data[index]);
      /*printf("jeng=%d \n",jeng);*/
      printf("16=%x \n",data[index]);
      printf("****************\n");

      fprintf(filewrite,"%d.A0000 C10080 C20000 T1%x T20008 C30\n",index,data[index
    }

  for(index=20001; index<=22000; index++)
    {
```

```
      /* intermed=1000*rand()/(RAND_MAX+1.0);*/
      /* intermed=rand()%(200000-2197+1)+2197;*/
      /*intermed=rand()%(208253-2198+1)+2198;*/
      intermed=rand()%(20000-211+1)+211;
      /*data[index]=-2197*log((intermed)/4000);*/
      data[index]=-164.00*log(intermed/20000.00);
      /* jeng=abs(data[index]);*/
      printf("time=%d \n",index);
      printf("rand=%d \n",intermed);
      printf("exp=%d \n",data[index]);
      /*printf("jeng=%d \n",jeng);*/
      printf("16=%x \nd",data[index]);


      printf("------------- \n");

      fprintf(filewrite,"%d.A0000 C10080 C20000 T1%x T20008 C30\n",index,data[index]);
    }



  fclose (filewrite);

  return 0;

}
```

Bibliography

[1] T. Ward, M. Barker, J. Breeden, K. Komisarcik, M. Pickar, D. Wark, and J. Wiggins, *Am. J. Phys.* **53**, 542 (1985).

[2] S.H. Neddermeyer and C.D. Anderson, *Phys. Rev.* **51**, 884 (1937).

[3] http://pdg.lbl.gov/2006/listings/s004.pdf

[4] http://pdg.lbl.gov/2006/listings/s008.pdf

[5] http://pdg.lbl.gov/2006/listings/s009.pdf

[6] http://pdg.lbl.gov/2006/reviews/cosmicrayrpp.pdf

[7] J. A. Simpson, *Ann. Rev. Nucl. Part. Sci.*, **33**, 323 (1983).

[8] H. Primakoff, *Rev. Mod. Phys.*, **31**, 802 (1959).

[9] J. C. Sens, *Phys. Rev.*, **113**, 679 (1959).

[10] Gerald Feinberg, Leon M. Lederman, *Ann. Rev. Nucl. Sci.*, **13**, 431 (1963).

[11] http://paw.web.cern.ch/paw/

[12] https://webafs3.cern.ch/wwwasdoc/hbook/H2Statistical-differences-between-histograms.html